

Cholesky Factorization With Symmetric Permutation Applied to Detecting and Precoding Spatially Multiplexed Data Streams

Katsutoshi Kusume, *Member, IEEE*, Michael Joham, *Member, IEEE*, Wolfgang Utschick, *Senior Member, IEEE*, and Gerhard Bauch, *Senior Member, IEEE*

Abstract—We study computationally efficient spatial multiplexing transmission techniques aiming at high spectral efficiency. Two nonlinear transmission schemes based on the minimum mean-squared error criterion are considered in this paper: a detection scheme also known as V-BLAST and a precoding scheme called Tomlinson–Harashima precoding. The nonlinear techniques are known to be more powerful than simple linear filters, however, a large complexity overhead results. Initial proposals for the nonlinear schemes require the complexity proportional to N^4 if the number of data streams is denoted by N . We propose to apply Cholesky factorization with symmetric permutation for finding a very simple and efficient algorithm that reduces the complexity by a factor of N . We conclude that the large performance advantage of the nonlinear detection and precoding schemes against their simple linear alternatives can be obtained without complexity overhead.

Index Terms—Cholesky factorization, decision feedback equalization (DFE), multiple-input multiple-output (MIMO), minimum-mean squared error (MMSE), successive interference cancellation (SIC), spatial multiplexing, symmetric permutation, Tomlinson–Harashima precoding (THP), vertical Bell Labs layered space-time (V-BLAST).

I. INTRODUCTION

VERY high spectral efficiency is expected in future wireless communication systems. It was shown in [1] that an enormous capacity increase can be achieved on flat *multiple-input multiple-output* (MIMO) channels compared to *single-input single-output* (SISO) channels in rich scattering environments. The capacity increase is linear with the number of transmit antennas unless it exceeds the number of receive antennas. To enable reliable communications in such systems, maximum-likelihood detection would be optimum; however, as the number of transmit antennas increases, the complexity of the receiver becomes prohibitive [2]. A number of research efforts have been made to develop low complexity methods to approach the large capacity promised by the MIMO channels, e.g.,

[3] and [4]. *Vertical Bell Labs layered space-time* (V-BLAST) architecture was proposed in [5] as detection scheme with low complexity. Independent data streams associated with different transmit antennas, called layers, are detected at the receiver by nulling out the interference of other layers in a successive manner. Also suggested is an optimum detection ordering which is of great importance for the *successive interference cancellation* (SIC).

The originally proposed V-BLAST in [5] calculates the nulling vector based on the *zero forcing* (ZF) criterion while in [6], [7] the *minimum-mean squared error* (MMSE) criterion is adopted to the V-BLAST architecture improving the performance. These detection schemes require computation of either a pseudo inverse (ZF V-BLAST) or an inverse (MMSE V-BLAST) at every step of the layer detection which is still computationally intensive for a large number of data streams. Many research activities have been dedicated to further reduce the complexity in the last years.

For the ZF criterion, computational reduction schemes have been proposed in [8] and [9] which are based on QR factorization with suboptimum detection ordering. In [10], a Cholesky factorization is utilized with reordering by unitary transformations leading to the optimum detection ordering. Similar contributions for the MMSE criterion based on QR factorization can be found in [11]–[13]. The ordering in [11] is suboptimum while in [12] the authors proposed an additional postsorting algorithm using unitary transformations to improve the performance. The contribution in [13] also utilizes unitary transformations for reordering. The authors in [14] proposed to apply a Cholesky factorization; however, they assume a known ordering. A fast recursive algorithm using the Sherman–Morrison formula was presented in [15]. This leads to the optimum solution and seems to be the most efficient algorithm proposed so far. Hence, we will compare the complexity of our proposed schemes with that of in [15].

While V-BLAST suffers from error propagation, its counterpart at transmitter, called spatial *Tomlinson–Harashima precoding* (THP) has been proposed in [16] to avoid the error propagation. THP was originally proposed for dispersive SISO channels in [17] and [18] to avoid inter-symbol interference. It moves the feedback filter of a *decision feedback equalization* (DFE) to the transmitter in order to circumvent error propagation. This requires that the channel is known at the transmitter (for THP with erroneous channel state information, see [19]). The same principle can be applied to resolve spatial interference in MIMO

Manuscript received June 13, 2005; revised October 16, 2006. This paper was presented in part at the IEEE Global Telecommunications Conference in November 2004 and at the IEEE International Conference on Communications in May 2005. The associate editor coordinating the review of this manuscript and approving it for publication was Dr. Luc Vandendorpe.

K. Kusume and G. Bauch are with DoCoMo Communications Laboratories Europe GmbH, 80687 Munich, Germany (e-mail: kusume@docomolab-euro.com; bauch@docomolab-euro.com).

M. Joham and W. Utschick are with the Associate Institute for Signal Processing, Munich University of Technology, 80290 Munich, Germany (e-mail: joham@tum.de; utschick@tum.de).

Digital Object Identifier 10.1109/TSP.2007.893978

as proposed in [16]. Note that all received signals must be cooperatively processed for the scheme of [16], i.e., linear combinations of the received signals must be computed, because the feedforward filter remains at the receiver. However, cooperative receive processing may not be possible in some scenarios, e.g., when the receive antennas belong to spatially separated users. It is also worth mentioning that applying *singular value decomposition* (SVD) is optimum in a scenario where cooperative receive processing is possible [20] while THP is not.

An interesting approach of spatial THP has been proposed in [21]–[24]. This approach moves not only the backward filter but also the forward filter to the transmitter. This architecture enables very simple receivers and more importantly, no signal processing among different receive antennas is necessary. A particularly interesting situation is that one transmitter is serving decentralized receivers or users in the downlink broadcast channel where no cooperation among receivers is possible. Unfortunately, the complexity of this approach at the transmitter becomes very high compared to linear transmit filters as in [25] for a large number of receivers.

We will show that computationally efficient algorithms for the above mentioned detection (V-BLAST) and precoding (THP) can be obtained by a new common framework: 1) strict derivation of optimum solution by explicitly including permutation matrix into system model, 2) applying Cholesky factorization with *symmetric permutation* to simplify the solution, and 3) extension to a suboptimum solution for further complexity reduction with a negligible performance loss. We first introduce our system model in Section II. Then, V-BLAST and THP are discussed in Section III and Section IV, respectively, where we briefly review the originally proposed algorithm, propose our new computationally efficient schemes, provide a complexity analysis, and give some numerical results. Since both successive detection and precoding schemes share many ideas, we will also discuss similarities and differences between these schemes in Section V. This paper is summarized in Section VI.

II. SYSTEM MODEL

We consider a discrete-time complex baseband model for a system with N_T transmit and N_R receive antennas. We assume narrowband signals, i.e., a nondispersive fading channel. The channel gain from transmit antenna $i = 1, \dots, N_T$ to receive antenna $j = 1, \dots, N_R$ is denoted by $h_{j,i}$. These channel taps are assumed to be i.i.d zero mean complex Gaussian variables of equal variance $E[|h_{j,i}|^2] = 1$ where $E[\cdot]$ denotes expectation. This assumption of independent paths holds if the antenna spacing is sufficiently large and the system is surrounded by rich scattering environments. The signal at receive antenna j can be expressed by $y_j = \sum_{i=1}^{N_T} h_{j,i}x_i + n_j$, where x_i and n_j , respectively, denote the signal transmitted from transmit antenna i and the additive noise at receive antenna j . By collecting y_j for N_R receive antennas, the received signals can be concisely expressed in matrix form

$$\mathbf{y} = \mathbf{H}\mathbf{x} + \mathbf{n} \quad (1)$$

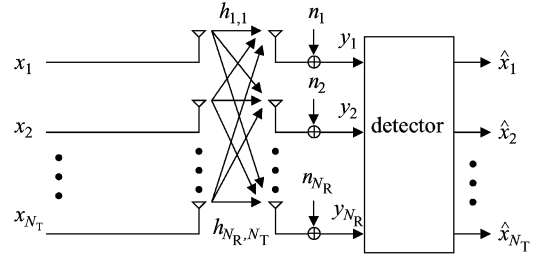


Fig. 1. System model for cooperatively detecting N_T data streams received by N_R antennas ($N_T \leq N_R$).

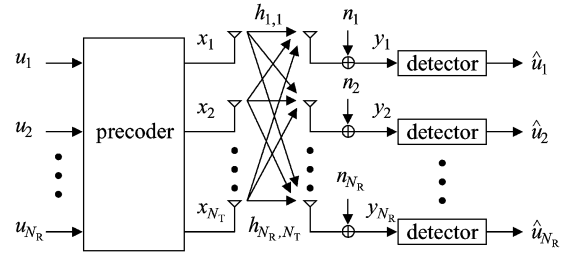


Fig. 2. System model for cooperatively precoding N_R data streams transmitted from N_T antennas ($N_R \leq N_T$).

where $[\mathbf{H}]_{j,i} = h_{j,i}$, $\mathbf{y} = [y_1, \dots, y_{N_R}]^T$, $\mathbf{x} = [x_1, \dots, x_{N_T}]^T$, $\mathbf{n} = [n_1, \dots, n_{N_R}]^T$, and $(\cdot)^T$ denotes transposition.

In this paper, we consider detection and precoding schemes for spatially multiplexing data streams. The detection scheme, also known as V-BLAST, is illustrated in Fig. 1. The N_T channel inputs x_i are simultaneously transmitted from N_T uncooperative antennas. The receiver cooperatively detects the N_T data streams using N_R antennas ($N_T \leq N_R$). We will describe our computationally efficient detection technique in Section III. In the case of the precoding scheme (Fig. 2), the N_R inputs u_j are cooperatively precoded and transmitted using N_T antennas ($N_T \geq N_R$). The signal at each receive antenna element is simply detected without any cooperation or knowledge of signals at other antennas. Our efficient implementation of the precoding technique will be explained in Section IV. Note that the two schemes complement each other: V-BLAST can be used in the uplink and THP in the downlink (see [26] for a SISO system).

By denoting the number of data streams by N and the number of information bits per data stream by M , the SNR per bit and per receive antenna is defined as

$$\frac{E_b}{N_0} \triangleq \frac{N_R E_s}{NM \text{tr}(\Phi_{nn})} \quad (2)$$

where “tr” denotes the trace of a matrix and the noise covariance matrix is defined as $\Phi_{nn} \triangleq E[\mathbf{n}\mathbf{n}^H]$, and $(\cdot)^H$ denotes Hermitian transpose of a matrix. In the case of uncorrelated noise, i.e., $\Phi_{nn} = \sigma_n^2 \mathbf{I}_{N_R}$, we have $E_b/N_0 = \frac{E_s}{NM\sigma_n^2}$. Note that $N = N_T$ for the detection scheme and $N = N_R$ for the precoding scheme. The average total transmit power E_s is expressed as $E_s \triangleq E[\mathbf{x}^H \mathbf{x}] = \text{tr}(\Phi_{xx})$, where $\Phi_{xx} \triangleq E[\mathbf{x}\mathbf{x}^H]$.

III. MMSE V-BLAST AND EQUIVALENT BLOCK DECISION FEEDBACK EQUALIZATION

We briefly review the MMSE V-BLAST algorithm. Let us first consider the error signal of a linear filter $\mathbf{F}^H \in \mathbb{C}^{N_T \times N_R}$ applied to the received vector \mathbf{y}

$$\boldsymbol{\varepsilon} \triangleq \mathbf{F}^H \mathbf{y} - \mathbf{x}. \quad (3)$$

The linear MMSE filter can be found with the *orthogonality principle* (see, e.g., [27]), that is $\mathbb{E}[\boldsymbol{\varepsilon} \mathbf{y}^H] = \mathbf{0}$. From (1) and (3), the solution is given by

$$\mathbf{F}_{\text{opt}}^H = \boldsymbol{\Phi}_{xy} \boldsymbol{\Phi}_{yy}^{-1} \quad (4)$$

where we defined $\boldsymbol{\Phi}_{xy} \triangleq \mathbb{E}[\mathbf{x} \mathbf{y}^H] = \boldsymbol{\Phi}_{xx} \mathbf{H}^H$ and $\boldsymbol{\Phi}_{yy} \triangleq \mathbb{E}[\mathbf{y} \mathbf{y}^H] = \mathbf{H} \boldsymbol{\Phi}_{xx} \mathbf{H}^H + \boldsymbol{\Phi}_{nn}$. Assuming that the covariance matrices are invertible, and with (3) and (4), the error covariance matrix $\boldsymbol{\Phi}_{\varepsilon\varepsilon} \triangleq \mathbb{E}[\boldsymbol{\varepsilon} \boldsymbol{\varepsilon}^H]$ can be expressed as

$$\boldsymbol{\Phi}_{\varepsilon\varepsilon} = \boldsymbol{\Phi}_{xx} - \boldsymbol{\Phi}_{xy} \boldsymbol{\Phi}_{yy}^{-1} \boldsymbol{\Phi}_{xy}^H = \left(\boldsymbol{\Phi}_{xx}^{-1} + \mathbf{H}^H \boldsymbol{\Phi}_{nn}^{-1} \mathbf{H} \right)^{-1} \quad (5)$$

where we applied the matrix inversion lemma¹ (see, e.g., [27]). Using the lemma, (4) may be rewritten as

$$\mathbf{F}_{\text{opt}}^H = \boldsymbol{\Phi}_{\varepsilon\varepsilon} \mathbf{H}^H \boldsymbol{\Phi}_{nn}^{-1}. \quad (6)$$

Notice that the error covariance matrix $\boldsymbol{\Phi}_{\varepsilon\varepsilon}$ plays an important role to determine the detection ordering for MMSE V-BLAST. Since the diagonal entries of $\boldsymbol{\Phi}_{\varepsilon\varepsilon}$ represent the *mean squared errors* (MSEs) of the respective channel inputs by definition, i.e., $\mathbb{E}[|x_i - \hat{x}_i|^2]$, $i = 1, \dots, N_T$, the channel input having the minimum diagonal entry of $\boldsymbol{\Phi}_{\varepsilon\varepsilon}$ can be seen as the most reliable one in MMSE sense. In SIC, the most reliable stream must be detected at the first stage to reduce the risk of error propagation. When denoting the detection ordering by the ordered set $\mathbb{K} \triangleq \{k_1, \dots, k_{N_T}\}$, then the k_1 th diagonal entry of $\boldsymbol{\Phi}_{\varepsilon\varepsilon}$ must be minimum. The respective filter $\mathbf{f}_{k_1}^H$ is the k_1 th row of \mathbf{F}^H . The output from $\mathbf{f}_{k_1}^H$ is quantized and decision is made to get \hat{x}_{k_1} . Assuming that this decision is correct ($\hat{x}_{k_1} = x_{k_1}$), the contribution of x_{k_1} on the received signal \mathbf{y} , i.e., x_{k_1} multiplied with the corresponding channel response, which is the k_1 th column of \mathbf{H} , is subtracted. At the second stage, since the k_1 th entry of \mathbf{x} has been detected, the k_1 th column of \mathbf{H} can be neglected; leading to an updated system only with $N_T - 1$ transmit antennas.

To generalize the procedure, the updated channel matrix \mathbf{H}_i is introduced for $i = 2, \dots, N_T$, where the k_1, \dots, k_{i-1} columns of \mathbf{H} are replaced by zeros and $\mathbf{H}_1 \triangleq \mathbf{H}$. At the i th stage, $\boldsymbol{\Phi}_{\varepsilon\varepsilon,i}$ and \mathbf{F}_i^H are calculated from (5) and (6) by replacing \mathbf{H} with \mathbf{H}_i . Then, the optimum filter calculation with ordering can be described as

$$k_i = \arg \min_{k \notin \{k_1, \dots, k_{i-1}\}} \mathbf{e}_k^T \boldsymbol{\Phi}_{\varepsilon\varepsilon,i} \mathbf{e}_k, \quad \text{and} \quad \mathbf{f}_{k_i}^H = \mathbf{e}_{k_i}^T \mathbf{F}_i^H \quad (7)$$

¹ $(\mathbf{A} + \mathbf{BCD})^{-1} = \mathbf{A}^{-1} - \mathbf{A}^{-1} \mathbf{B} (\mathbf{D} \mathbf{A}^{-1} \mathbf{B} + \mathbf{C}^{-1}) \mathbf{D} \mathbf{A}^{-1}$.

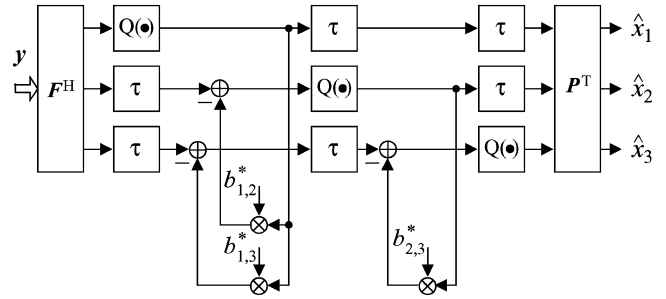


Fig. 3. Example of block DFE structure for three data streams. \mathbf{P}^T is a permutation matrix recovering original ordering of data streams which may be changed by the forward filter \mathbf{F}^H . τ denotes delay.

where \mathbf{e}_k is the k th column of the identity matrix \mathbf{I}_{N_T} . The MMSE V-BLAST repeats the procedure in (7) N_T times; thus, it requires the matrix inverse calculation in (5) for each channel input. That becomes computationally expensive for large N_T , since we end up with $O(N_T^4)$.

Note that it is also possible to formulate the V-BLAST algorithm in a slightly different manner. That is to update \mathbf{H}_i by removing the columns which correspond to the already detected channel inputs, instead of replacing them by zeros. This naturally leads to the lower complexity than the above formulation with the same result (it still remains of the same order $O(N_T^4)$, though). Nevertheless, we adopt the above formulation due to the convenience to prove later that our proposed algorithm is equivalent to the original MMSE V-BLAST with greatly reduced complexity.

A. Optimum MMSE DFE Applying Cholesky Factorization With Symmetric Permutation

We derive our new algorithm based on a specific receiver structure. As discussed, e.g., in [14] and [28], it is useful to describe the SIC architecture by a pair of forward and backward block filters with a certain constraint on the backward filter structure. In contrast to the frequently used system model, e.g., in [14] and [28], we propose to include the detection order *explicitly* in the system model for the filter derivation. An example of three data streams is illustrated in Fig. 3. There are three main components in this figure which are subject to optimization. The forward filter \mathbf{F}^H is applied to the received signal \mathbf{y} . With proper delays, each output signal from the forward filter is detected by the quantizer $Q(\cdot)$ and subtracted from the rest of the data streams in a successive manner after being multiplied with the respective feedback filter coefficient, e.g., $b_{1,2}^*$, where $(\cdot)^*$ denotes complex conjugation. The backward filter coefficients can be stored in a matrix $\mathbf{B}^H \in \mathbb{C}^{N_T \times N_T}$ that must be unit lower triangular² so that $\mathbf{B}^H - \mathbf{I}_{N_T}$ becomes strictly lower triangular. Then, its outputs are not subtracted from the already detected signals (cf. Fig. 3). This causality constraint is necessary to describe the SIC procedure. Finally, the original ordering of data streams is recovered by a permutation matrix \mathbf{P}^T . Due to the permutation \mathbf{P}^T which we explicitly included, as we will see, the forward filter \mathbf{F}^H resulting from the optimization includes the respective \mathbf{P} expressing the detection ordering.

²Unit lower triangular matrices are lower triangular matrices with ones along the main diagonal.

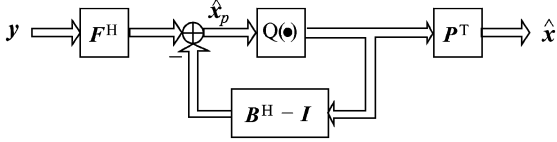


Fig. 4. System model for deriving the MMSE block DFE taking into account detection ordering represented by permutation matrix \mathbf{P} .

The permutation matrix can be written in a general form as $\mathbf{P} \triangleq \sum_{i=1}^{N_T} \mathbf{e}_i \mathbf{e}_{k_i}^T \in \{0, 1\}^{N_T \times N_T}$ to express the detection order $\mathbb{K} = \{k_1, \dots, k_{N_T}\}$. The transpose of \mathbf{P} restores the original ordering, i.e., $\mathbf{P}^T \mathbf{P} = \mathbf{P} \mathbf{P}^T = \mathbf{I}_{N_T}$. A compact general system model for the optimization is illustrated in Fig. 4.

Instead of $\hat{\mathbf{x}}$, we optimize the estimate $\hat{\mathbf{x}}_p$ (cf. Fig. 4) which can be expressed as

$$\hat{\mathbf{x}}_p = \mathbf{F}^H \mathbf{y} - (\mathbf{B}^H - \mathbf{I}) \mathbf{P} \hat{\mathbf{x}}.$$

The desired signal for $\hat{\mathbf{x}}_p$ is the channel input \mathbf{x} permuted by \mathbf{P} . Assuming that decisions made prior to every detection stage are correct ($\hat{\mathbf{x}} = \mathbf{x}$), the error vector is written as

$$\boldsymbol{\varepsilon}_p \triangleq \mathbf{P} \mathbf{x} - \hat{\mathbf{x}}_p = \mathbf{B}^H \mathbf{P} \mathbf{x} - \mathbf{F}^H \mathbf{y}. \quad (8)$$

Then, the MSE reads as

$$\varphi_p \triangleq \mathbb{E} [\|\boldsymbol{\varepsilon}_p\|_2^2] = \text{tr} (\boldsymbol{\Phi}_{\boldsymbol{\varepsilon}\boldsymbol{\varepsilon}}^{(p)}) \quad (9)$$

where the error covariance matrix is defined as $\boldsymbol{\Phi}_{\boldsymbol{\varepsilon}\boldsymbol{\varepsilon}}^{(p)} \triangleq \mathbb{E} [\boldsymbol{\varepsilon}_p \boldsymbol{\varepsilon}_p^H]$.

Our goal is to jointly optimize the forward and backward filters by minimizing the MSE φ_p . As the backward filter must be strictly lower triangular, our optimization problem is

$$\{\mathbf{F}_{\text{opt}}, \mathbf{B}_{\text{opt}}\} = \arg \min_{\{\mathbf{F}, \mathbf{B}\}} \varphi_p$$

$$\text{s.t. : } \mathbf{e}_i^T (\mathbf{B}^H - \mathbf{I}_{N_T}) \mathbf{S}_i^T = \mathbf{0}_{N_T - i + 1 \times 1}, \quad i = 1, \dots, N_T \quad (10)$$

where the selection matrix cuts out the last $N_T - i + 1$ elements of an N_T -dimensional vector

$$\mathbf{S}_i \triangleq [\mathbf{0}_{N_T - i + 1 \times i - 1}, \mathbf{I}_{N_T - i + 1}] \in \{0, 1\}^{N_T - i + 1 \times N_T}. \quad (11)$$

Note that the constraint in (10) is defined for every row of the backward filter so that its upper triangular part must be zero. The constrained optimization problem in (10) can be solved using Lagrangian multipliers (see, e.g., [29] and [30]), and we get the solution for the forward and backward filters (see Appendix I)

$$\begin{aligned} \mathbf{F}_{\text{opt}}^H &= \sum_{i=1}^{N_T} \mathbf{e}_i \mathbf{e}_i^T \mathbf{S}_i^T (\mathbf{S}_i \mathbf{P} \boldsymbol{\Phi}_{\boldsymbol{\varepsilon}\boldsymbol{\varepsilon}}^{-1} \mathbf{P}^T \mathbf{S}_i^T)^{-1} \mathbf{S}_i \mathbf{P} \mathbf{H}^H \boldsymbol{\Phi}_{nn}^{-1}, \\ \mathbf{B}_{\text{opt}}^H &= \sum_{i=1}^{N_T} \mathbf{e}_i \mathbf{e}_i^T \mathbf{S}_i^T (\mathbf{S}_i \mathbf{P} \boldsymbol{\Phi}_{\boldsymbol{\varepsilon}\boldsymbol{\varepsilon}}^{-1} \mathbf{P}^T \mathbf{S}_i^T)^{-1} \mathbf{S}_i \mathbf{P} \boldsymbol{\Phi}_{\boldsymbol{\varepsilon}\boldsymbol{\varepsilon}}^{-1} \mathbf{P}^T \end{aligned} \quad (12)$$

respectively. As can be observed from (12), the filters are determined row by row, each of which requires one matrix inverse as it is the case for the MMSE V-BLAST. Note that the minimization of every individual MSE, i.e., $\min_{\mathbf{F}, \mathbf{B}} \mathbf{e}_k^T \boldsymbol{\Phi}_{\boldsymbol{\varepsilon}\boldsymbol{\varepsilon}}^{(p)} \mathbf{e}_k, \forall k$, leads

to the same solution as in (12) for sum MSE minimization, since the k th MSE $\mathbf{e}_k^T \boldsymbol{\Phi}_{\boldsymbol{\varepsilon}\boldsymbol{\varepsilon}}^{(p)} \mathbf{e}_k$ only depends on the k th rows of \mathbf{F}^H and \mathbf{B}^H [cf. (8)].

The MSE φ_p using the results in (12) can be written as (see Appendix I)

$$\varphi_p = \sum_{i=1}^{N_T} \mathbf{e}_{k_i}^T (\boldsymbol{\Pi}_i \boldsymbol{\Phi}_{\boldsymbol{\varepsilon}\boldsymbol{\varepsilon}}^{-1} \boldsymbol{\Pi}_i)^+ \mathbf{e}_{k_i} \quad (13)$$

where we defined

$$\boldsymbol{\Pi}_i \triangleq \mathbf{P}^T \mathbf{S}_i^T \mathbf{S}_i \mathbf{P} = \mathbf{I}_{N_T} - \sum_{j=1}^{i-1} \mathbf{e}_{k_j} \mathbf{e}_{k_j}^T. \quad (14)$$

Because the detection order should be chosen as to minimize the MSE φ_p , we can write

$$\{k_1, \dots, k_{N_T}\}_{\text{opt}} = \arg \min_{\{k_1, \dots, k_{N_T}\}} \sum_{i=1}^{N_T} \mathbf{e}_{k_i}^T (\boldsymbol{\Pi}_i \boldsymbol{\Phi}_{\boldsymbol{\varepsilon}\boldsymbol{\varepsilon}}^{-1} \boldsymbol{\Pi}_i)^+ \mathbf{e}_{k_i}. \quad (15)$$

Remark 3.1: We see that $\boldsymbol{\Pi}_i$ is independent of k_i, \dots, k_{N_T} from (14). In this view, we obtain the MMSE V-BLAST of (7) if we minimize each summand separately, i.e., k_i is chosen under the assumption that k_1, \dots, k_{i-1} are fixed. Obviously, the ordering resulting from (15) is different from the MMSE V-BLAST ordering in (7), in general.

Next, we show that the results in (12) can be greatly simplified by the following equation:

$$\mathbf{P} \boldsymbol{\Phi}_{\boldsymbol{\varepsilon}\boldsymbol{\varepsilon}} \mathbf{P}^T = \mathbf{L} \mathbf{D} \mathbf{L}^H \quad (16)$$

where $\mathbf{L} \in \mathbb{C}^{N_T \times N_T}$ and $\mathbf{D} \in \mathbb{R}^{N_T \times N_T}$ are a unit lower triangular matrix and a diagonal matrix, respectively. Equation (16) is called the Cholesky factorization with symmetric permutation [31]. The factorization can be computed since $\boldsymbol{\Phi}_{\boldsymbol{\varepsilon}\boldsymbol{\varepsilon}}$ is Hermitian and also positive definite. With (16), the forward and backward filters in (12) reduce to (see Appendix I)

$$\mathbf{F}_{\text{opt}}^H = \mathbf{D} \mathbf{L}^H \mathbf{P} \mathbf{H}^H \boldsymbol{\Phi}_{nn}^{-1} \quad \text{and} \quad \mathbf{B}_{\text{opt}}^H = \mathbf{L}^{-1}. \quad (17)$$

This is a significant reduction of computational complexity compared with (12). One factorization of $\boldsymbol{\Phi}_{\boldsymbol{\varepsilon}\boldsymbol{\varepsilon}}$ in (16) and the inversion of the triangular matrix \mathbf{L} suffice instead of N_T times matrix inversions. Notice that applying (16) to (12) is the straightforward idea that is the consequence of the permutation matrix \mathbf{P}^T which we explicitly introduced in the system model (cf. Figs. 3 and 4). Furthermore, we see that the resulting forward filter structure makes sense as it applies the matched filter $\mathbf{H}^H \boldsymbol{\Phi}_{nn}^{-1}$ followed by the detection ordering optimization \mathbf{P} , the interference suppression \mathbf{L}^H , and the gain control \mathbf{D} before the decision device.

The results also simplify the error covariance matrix as follows (see Appendix I):

$$\boldsymbol{\Phi}_{\boldsymbol{\varepsilon}\boldsymbol{\varepsilon}}^{(p)} = \mathbf{D} \triangleq \text{diag} (d_1, \dots, d_{N_T}). \quad (18)$$

Remark 3.2: d_i is the MSE of the i th detected channel input x_{k_i} .

TABLE I
DFE DETECTION USING CALCULATED FILTERS AND ORDERING

$$\begin{aligned} \hat{\mathbf{x}}_p &= \mathbf{F}^H \mathbf{y}, \mathbf{B}^H = \mathbf{B}^H - \mathbf{I}_{N_T} \text{ (strictly triangular)} \\ \text{for } i &= 1, \dots, N_T \\ \hat{\mathbf{x}}_p(i) &= \mathbf{Q}(\hat{\mathbf{x}}_p(i) - \mathbf{B}^H(i, :)\hat{\mathbf{x}}_p) \\ \hat{\mathbf{x}} &= \mathbf{P}^T \hat{\mathbf{x}}_p \end{aligned}$$

Equation (18) means that the resulting error signal becomes uncorrelated and the ordering optimization in (15) can be rewritten as [also see (9) and (13)]

$$\{k_1, \dots, k_{N_T}\}_{\text{opt}} = \arg \min_{\{k_1, \dots, k_{N_T}\}} \sum_{i=1}^{N_T} d_i. \quad (19)$$

Recall Remark 3.1 that minimizing each summand of (15) separately yields the MMSE V-BLAST of (7). Thus, the MMSE V-BLAST in (7) is equivalent to

$$k_i = \arg \min_{k \notin \{k_1, \dots, k_{i-1}\}} d_k. \quad (20)$$

Note that (20) leads to different orderings from (19) in general (cf. Remark 3.1). We can conclude that a successive algorithm computing (16) by minimizing the diagonal entries of \mathbf{D} for fixed previous indices $\{k_1, \dots, k_{i-1}\}$ leads to the optimum MMSE V-BLAST ordering as in (7).

In [31, pp. 148], a successive algorithm to compute (16) is presented. It is based on the following partitioning:

$$\begin{aligned} \mathbf{P}_1 \Phi_{\varepsilon\varepsilon,1} \mathbf{P}_1^T &= \begin{bmatrix} d_1 & \boldsymbol{\ell}_1^H \\ \boldsymbol{\ell}_1 & \Psi_1 \end{bmatrix} \\ &= \begin{bmatrix} 1 & \mathbf{0}^T \\ \boldsymbol{\ell}_1/d_1 & \mathbf{I} \end{bmatrix} \begin{bmatrix} d_1 & \mathbf{0}^T \\ \mathbf{0} & \Phi_{\varepsilon\varepsilon,2} \end{bmatrix} \begin{bmatrix} 1 & \boldsymbol{\ell}_1^H/d_1 \\ \mathbf{0} & \mathbf{I} \end{bmatrix} \end{aligned}$$

where $\Phi_{\varepsilon\varepsilon,1} \triangleq \Phi_{\varepsilon\varepsilon}$, and $\Phi_{\varepsilon\varepsilon,2} \triangleq \Psi_1 - \boldsymbol{\ell}_1 \boldsymbol{\ell}_1^H / d_1$. This procedure can be repeated to complete the factorization. The algorithm in [31] finds the *maximum* diagonal entry at each step to enhance numerical stability for semidefinite matrices. That means, for example, at the first step shown above, the permutation \mathbf{P}_1 is chosen such that d_1 is the *maximum* entry among all the diagonal ones. However, since the diagonal entries in our system represent the MSEs of the ordered channel inputs (recall Remark 3.2: d_1 is the MSE of the channel input x_{k_1} detected first), we propose to choose the *minimum* diagonal entry (opposite to [31]), then we equivalently achieve MMSE at each iteration. As discussed above, this procedure is equal to the MMSE V-BLAST algorithm, but we do not require the multiple matrix inversions. Our proposed algorithm is summarized as a pseudo code in Tables I and II for the detection procedure and the filter calculation, respectively.

B. Suboptimum MMSE DFE Applying Cholesky Factorization With Symmetric Permutation

The proposed optimum ordered Cholesky approach described in the previous section requires the computation of the matrix inverse in (5) to determine the error covariance matrix (also see the first line of Table II). To avoid this inversion, we compute the modified factorization as

$$\mathbf{P} \Phi_{\varepsilon\varepsilon}^{-1} \mathbf{P}^T = \mathbf{L}^H \mathbf{D}' \mathbf{L}' \quad (21)$$

TABLE II
CALCULATION OF DFE FILTERS WITH OPTIMUM DETECTION ORDERING

$$\begin{aligned} 1: & \Phi_{\varepsilon\varepsilon} = (\Phi_{xx}^{-1} + \mathbf{H}^H \Phi_{nn}^{-1} \mathbf{H})^{-1}, \mathbf{P} = \mathbf{I}_{N_T}, \mathbf{D} = \mathbf{0}_{N_T} \\ 2: & \text{for } i = 1, \dots, N_T \\ 3: & q = \arg \min_{q'=i, \dots, N_T} \Phi_{\varepsilon\varepsilon}(q', q') \\ & \mathbf{P}_i = \mathbf{I}_{N_T} \text{ whose } i\text{-th and } q\text{-th rows are exchanged} \\ & \mathbf{P} = \mathbf{P}_i \mathbf{P}, \Phi_{\varepsilon\varepsilon} = \mathbf{P}_i \Phi_{\varepsilon\varepsilon} \mathbf{P}_i^T \\ & \mathbf{D}(i, i) = \Phi_{\varepsilon\varepsilon}(i, i), \Phi_{\varepsilon\varepsilon}(i:N_T, i) = \Phi_{\varepsilon\varepsilon}(i:N_T, i) / \mathbf{D}(i, i) \\ & \text{for } j = i + 1, \dots, N_T \\ & \Phi_{\varepsilon\varepsilon}(j:N_T, j) = \Phi_{\varepsilon\varepsilon}(j:N_T, j) - \Phi_{\varepsilon\varepsilon}(j:N_T, i) \Phi_{\varepsilon\varepsilon}^*(j, i) \mathbf{D}(i, i) \\ & \Phi_{\varepsilon\varepsilon}(j, j:N_T) = \Phi_{\varepsilon\varepsilon}(j:N_T, j)^H \\ & \mathbf{L} = \text{lower triangular of } \Phi_{\varepsilon\varepsilon} \\ 11: & \mathbf{B}^H = \mathbf{L}^{-1}, \mathbf{F}^H = \mathbf{D} \mathbf{L}^H \mathbf{P} \mathbf{H}^H \Phi_{nn}^{-1} \end{aligned}$$

TABLE III
CALCULATION OF DFE FILTERS WITH SUBOPTIMUM ORDERING

$$\begin{aligned} 1: & \Phi_{\varepsilon\varepsilon}^{-1} = \Phi_{xx}^{-1} + \mathbf{H}^H \Phi_{nn}^{-1} \mathbf{H}, \mathbf{P} = \mathbf{I}_{N_T}, \mathbf{D} = \mathbf{0}_{N_T} \\ 2: & \text{for } i = N_T, \dots, 1 \\ 3: & q = \arg \min_{q'=1, \dots, i} \Phi_{\varepsilon\varepsilon}^{-1}(q', q') \\ & \mathbf{P}_i = \mathbf{I}_{N_T} \text{ whose } i\text{-th and } q\text{-th rows are exchanged} \\ & \mathbf{P} = \mathbf{P}_i \mathbf{P}, \Phi_{\varepsilon\varepsilon}^{-1} = \mathbf{P}_i \Phi_{\varepsilon\varepsilon}^{-1} \mathbf{P}_i^T \\ & \mathbf{D}(i, i) = \Phi_{\varepsilon\varepsilon}^{-1}(i, i), \Phi_{\varepsilon\varepsilon}^{-1}(1:i, i) = \Phi_{\varepsilon\varepsilon}^{-1}(1:i, i) / \mathbf{D}(i, i) \\ & \text{for } j = 1, \dots, i - 1 \\ & \Phi_{\varepsilon\varepsilon}^{-1}(1:j, j) = \Phi_{\varepsilon\varepsilon}^{-1}(1:j, j) - \Phi_{\varepsilon\varepsilon}^{-1}(1:j, i) \Phi_{\varepsilon\varepsilon}^{-1}(i, j) \mathbf{D}(i, i) \\ & \Phi_{\varepsilon\varepsilon}^{-1}(j, 1:j) = \Phi_{\varepsilon\varepsilon}^{-1}(1:j, j)^H \\ & \mathbf{L}^H = \text{upper triangular of } \Phi_{\varepsilon\varepsilon}^{-1} \\ 11: & \mathbf{B}^H = \mathbf{L}, \mathbf{F}^H = \mathbf{D}^{-1} \mathbf{L}'^{-H} \mathbf{P} \mathbf{H}^H \Phi_{nn}^{-1} \end{aligned}$$

where \mathbf{L}' and \mathbf{D}' are a lower triangular matrix and a diagonal matrix, respectively. To avoid possible confusion, we note that $\Phi_{\varepsilon\varepsilon}^{-1} = \Phi_{xx}^{-1} + \mathbf{H}^H \Phi_{nn}^{-1} \mathbf{H}$ requires one less matrix inversion comparing to $\Phi_{\varepsilon\varepsilon}$. Since we can rewrite (21) as [cf. (16)]

$$\mathbf{P} \Phi_{\varepsilon\varepsilon} \mathbf{P}^T = \mathbf{L}'^{-1} \mathbf{D}'^{-1} \mathbf{L}'^{-H} \quad (22)$$

and the inverse of any unit lower triangular matrix is again unit lower triangular [31, pp. 93], we can reuse the result of the optimum solution in (17) to end up with

$$\mathbf{F}_{\text{subopt}}^H = \mathbf{D}'^{-1} \mathbf{L}'^{-H} \mathbf{P} \mathbf{H}^H \Phi_{nn}^{-1} \text{ and } \mathbf{B}_{\text{subopt}}^H = \mathbf{L}'. \quad (23)$$

The algorithm for the filter calculation is summarized as a pseudo code in Table III. We note that the suboptimum solution cannot be computed by the optimum algorithm in Table II. If, nevertheless, the algorithm in Table II is used for $\Phi_{\varepsilon\varepsilon}^{-1}$, we get $\mathbf{P} \Phi_{\varepsilon\varepsilon}^{-1} \mathbf{P}^T = \mathbf{L}' \mathbf{D}' \mathbf{L}'^H$ [cf. (21)] and the corresponding backward filter, consequently, becomes upper triangular ($\mathbf{B}^H = \mathbf{L}'^H$) that contradicts the constraint in (10). This observation shows that the inversion at the beginning of Table II cannot be dropped.

In the following, we explain why this algorithm is suboptimum. The error covariance matrix of the suboptimum solution reads as $\Phi_{\varepsilon\varepsilon}^{(p)} = \mathbf{D}'^{-1} = \text{diag}(d_1'^{-1}, \dots, d_{N_T}'^{-1})$.

Remark 3.3: $d_i'^{-1}$ is the MSE of the i th detected channel input x_{k_i} .

The ordering optimization in (15) can now be rewritten as $\{k_1, \dots, k_{N_T}\}_{\text{opt}} = \arg \min_{\{k_1, \dots, k_{N_T}\}} \sum_{i=1}^{N_T} d_i'^{-1}$. Thus, the solution would be optimum for successive detection if the following criterion were possible: $k_i = \arg \min_{k \notin \{k_1, \dots, k_{i-1}\}} d_k'^{-1}$

TABLE IV
COMPLEXITY COMPARISON OF DIFFERENT DETECTION SCHEMES

	V-BLAST (from [15])	fast V-BLAST in [15]	optimum Cholesky	suboptimum Cholesky
multiplications	$\frac{9}{4}N_T^4 + \frac{4}{3}N_T^3 N_R + \frac{29}{6}N_T^2 + \frac{5}{2}N_T^2 N_R$	$\frac{1}{6}N_T^2(4N_T + 18N_R)$	$\frac{1}{6}N_T^2(5N_T + 3N_R)$	$\frac{1}{6}N_T^2(2N_T + 3N_R)$
additions	$\frac{9}{4}N_T^4 + \frac{4}{3}N_T^3 N_R + \frac{29}{6}N_T^2 + \frac{5}{2}N_T^2 N_R$	$\frac{1}{6}N_T^2(3N_T + 15N_R)$	$\frac{1}{6}N_T^2(5N_T + 3N_R)$	$\frac{1}{6}N_T^2(2N_T + 3N_R)$

[cf. (15) and (20)]. However, this is not the case since the suboptimum algorithm in Table III is based on the repeated application of the following partitioning:

$$\begin{aligned} \mathbf{P}_{N_T} \Phi_{\varepsilon\varepsilon, N_T}^{-1} \mathbf{P}_{N_T}^T &= \begin{bmatrix} \Psi'_{N_T} & \ell'_{N_T} \\ \ell'^H_{N_T} & d'_{N_T} \end{bmatrix} \\ &= \begin{bmatrix} \mathbf{I} & \ell'_{N_T}/d'_{N_T} \\ \mathbf{0}^T & 1 \end{bmatrix} \begin{bmatrix} \Phi_{\varepsilon\varepsilon, N_T-1}^{-1} & \mathbf{0} \\ \mathbf{0}^T & d'_{N_T} \end{bmatrix} \\ &\quad \times \begin{bmatrix} \mathbf{I} & \mathbf{0} \\ \ell'^H_{N_T}/d'_{N_T} & 1 \end{bmatrix} \end{aligned}$$

where $\Phi_{\varepsilon\varepsilon, N_T}^{-1} \triangleq \Phi_{\varepsilon\varepsilon}^{-1}$ and $\Phi_{\varepsilon\varepsilon, N_T-1}^{-1} \triangleq \Psi'_{N_T} - \ell'_{N_T} \ell'^H_{N_T} / d'_{N_T}$. Clearly, we must start the factorization by choosing the channel input detected last (recall Remark 3.3) that is undesired and in the opposite direction compared to the optimum solution. This explains the suboptimality. Furthermore, we observed that the general criterion at each iteration, $k_i = \arg \min_{k \notin \{k_{i+1}, \dots, k_{N_T}\}} d'_k{}^{-1}$, results in poor overall performance. That is because the criterion leads to the improvement of the layers detected later, but it does not bring the improvement to the earlier detected layers which limit the overall performance [32]. Therefore, we propose the following criterion as can be found in Table III:

$$k_i = \arg \max_{k \notin \{k_{i+1}, \dots, k_{N_T}\}} d'_k{}^{-1} = \arg \min_{k \notin \{k_{i+1}, \dots, k_{N_T}\}} d'_k.$$

Starting from the last detected layer, at each iteration we choose the worst layer, which benefits most from the SIC, and the better layers are detected earlier so that the overall performance should not be limited by the earlier detected layers. However, that does not always lead to the optimum detection ordering.

C. Complexity Analysis

As discussed in Section I the complexity reduction of the original V-BLAST has been intensively studied in the last years, e.g., [8]–[15]. We compare the computational complexity of the proposed algorithms with that of the fast recursive algorithm [15] which is the most efficient algorithm proposed so far. The analysis is performed under the assumption of uncorrelated input and noise, i.e., $\Phi_{xx} = \sigma_x^2 \mathbf{I}_{N_T}$ and $\Phi_{nn} = \sigma_n^2 \mathbf{I}_{N_R}$. Since all processing is conducted on complex values, multiplications and additions refer to complex operations. The complexity comparison is summarized in Table IV neglecting the terms below the third order for brevity. If $N_T = N_R$, then the speedups of the proposed optimum solution over the fast recursive V-BLAST in the number of multiplications and additions are 2.75 and 2.25, respectively. Our suboptimum solution is even faster, in a factor of 4.40 and 3.60 for multiplications and additions, respectively, with a negligible performance loss

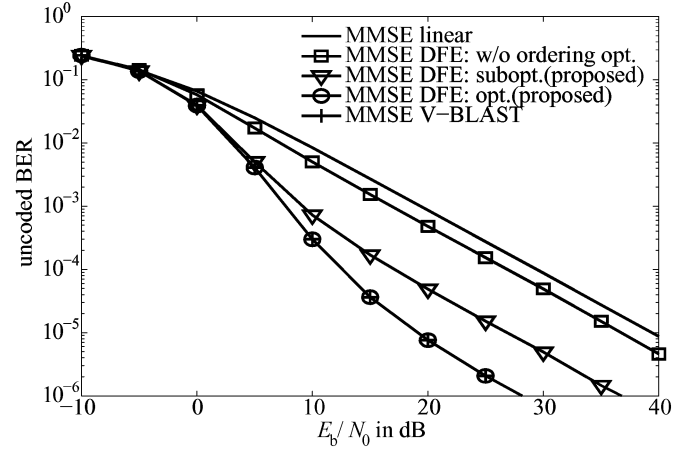


Fig. 5. Uncoded BER performance of a system with $N_T = N_R = 4$ antennas.

as illustrated in the next section. If $N_T < N_R$, which is a usual case (e.g., $N_T = 8$, $N_R = 12$ in [5]), the advantages of our proposed solutions are larger as we can see from Table IV that the complexity of our solutions are less sensitive to N_R in a factor of 6 and 5, for multiplications and additions, respectively, comparing to the fast V-BLAST. We note that the complexity of our suboptimum solution is roughly that of the simple linear MMSE filter (not even SIC!) in (6) whose complexity is due to the computation of $\Phi_{\varepsilon\varepsilon}$ and it is given by (22) without permutation ($\mathbf{P} = \mathbf{I}$).

D. Numerical Results

Computer simulations are performed to evaluate the uncoded BER over E_b/N_0 [see (2)]. The channel input and the noise are assumed white. The frame length of 10^3 information bits are QPSK modulated. A quasi static channel is considered. The performance is averaged over a large number of channel realizations. The channel and SNR are assumed to be perfectly known at the receiver. Fig. 5 shows the uncoded BER performance of a system with $N_T = N_R = 4$ antennas both at the transmitter and the receiver. It can be observed that our optimum MMSE DFE achieves the same performance as the MMSE V-BLAST, but with significantly lower complexity. The significance of the detection order can be also observed. Our suboptimum DFE does not approach the optimum performance in the low uncoded BER region, but almost has no performance degradation in the uncoded BER of, e.g., 10^{-2} which is a practical operating point in coded transmission. The performance loss due to the suboptimality of the ordering optimization is further investigated. We observed that the loss of our suboptimum solution in a wide range of the number of antennas for $N_T = N_R$ is below 0.4 dB at an uncoded BER of 10^{-2} .

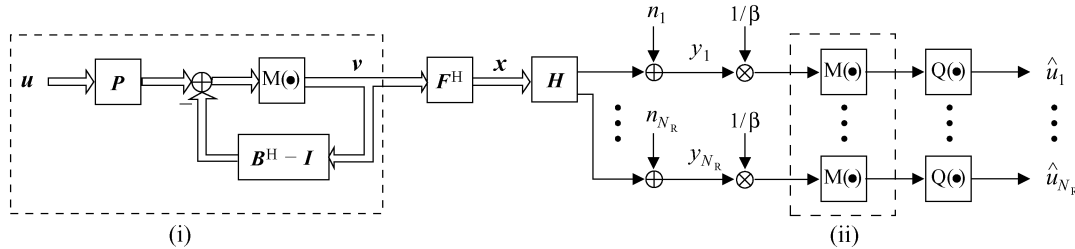


Fig. 6. Block diagram of THP transmission. Also see the alternative linear representations of the modulo operators of the sub-blocks (i) and (ii) in Fig. 8.

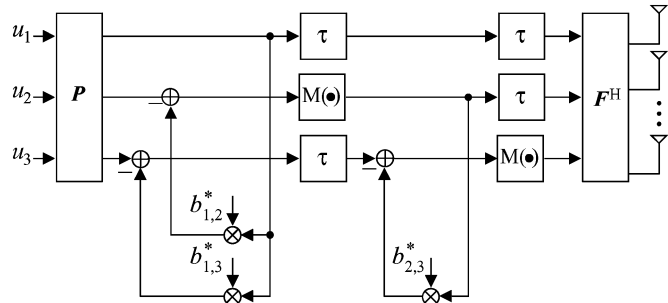


Fig. 7. Example of THP structure for three data streams. \mathbf{P} is a permutation matrix changing the ordering of data streams where the forward filter \mathbf{F}^H is responsible for restoring the original ordering. τ denotes delay.

IV. MMSE TOMLINSON–HARASHIMA PRECODING

We first review the MMSE THP scheme presented in [24] with some modifications. The overall system structure is illustrated as a block diagram in Fig. 6 where the permutation matrix \mathbf{P} is additionally introduced to the system model in [24]. We assume that the input symbol u_j , $j = 1, \dots, N_R$, is taken from a square QAM constellation and we define the set $\mathbb{A} \triangleq \{\alpha_M^{-1}(x + jy) | x, y \in \{\pm 1, \pm 3, \dots, \pm(M-1)\}\}$ where $M \triangleq 2^b$ ($b \in \mathbb{N}$) is the number of bits per symbol and $\alpha_M \in \mathbb{R}_+$ is chosen so that the average symbol energy is unity, i.e., $\mathbb{E}[|u_j|^2] = 1, \forall j$. For instance, $\alpha_2 = \sqrt{2}$, $\alpha_4 = \sqrt{10}$, and $\alpha_6 = \sqrt{42}$ for 4QAM (QPSK), 16QAM, and 64QAM, respectively. The input signal vector $\mathbf{u} \triangleq [u_1, \dots, u_{N_R}]^T$ is reordered as $\mathbf{Pu} \in \mathbb{C}^{N_R}$ which is iteratively filtered by the backward filter and also by the modulo operator where $\mathbf{P} \triangleq \sum_{j=1}^{N_R} \mathbf{e}_j \mathbf{e}_{k_j}^T \in \{0, 1\}^{N_R \times N_R}$ and the precoding ordering is denoted by the ordered set $\{k_1, \dots, k_{N_R}\}$. The precoding procedure may be better understood by an example illustrated in Fig. 7 for three data streams. With proper delays each data stream is multiplied with the feedback filter coefficients, e.g., $b_{1,2}^*$, and subtracted from the other data streams to cancel out the interference. Since this iterative feedback process would increase the signal power significantly, the modulo operator is introduced to reduce the signal power. The modulo operator is defined for a complex variable c as

$$M(c) \triangleq M'(\text{Re}\{c\}) + jM'(\text{Im}\{c\})$$

$$\text{where } M'(r) \triangleq r - \left\lfloor \frac{\alpha_M}{2M} r + \frac{1}{2} \right\rfloor \frac{2M}{\alpha_M}, \quad r \in \mathbb{R} \quad (24)$$

and the floor operator $\lfloor \cdot \rfloor$ rounds the argument to the nearest integer towards minus infinity. Apparently, the output signal v_j from $M(\cdot)$ is an element of the set $\mathbb{M} \triangleq \{x + jy | x, y \in$

TABLE V
ITERATIVE PRECODING PROCEDURE WITH ORDERING

$$\begin{aligned} \mathbf{v} &= \mathbf{P}\mathbf{u}, \quad \mathbf{B}^H = \mathbf{B}^H - \mathbf{I}_{N_R} \text{ (strictly triangular)} \\ \text{for } i &= 1, \dots, N_R \\ \mathbf{v}(i) &= M(\mathbf{v}(i) - \mathbf{B}^H(i, :)\mathbf{v}) \\ \mathbf{x} &= \mathbf{F}^H \mathbf{v} \end{aligned}$$

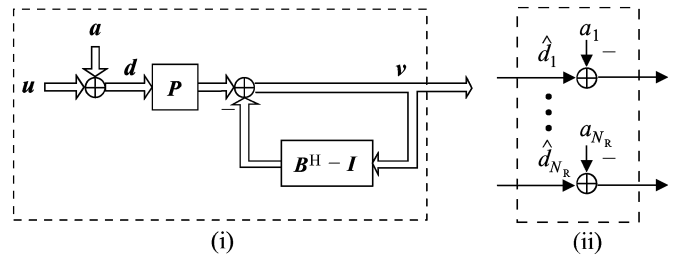


Fig. 8. Alternative linear representations of modulo operators in Fig. 6.

$[-M/\alpha_M, M/\alpha_M]\}$ and assuming that v_j is uniformly distributed, the variance is $\sigma_{v_j}^2 = \frac{2M^2}{3\alpha_M^2}$ for $j \neq 1$ and $\sigma_{v_1}^2 = 1$. We denote $\sigma_v^2 \triangleq \frac{2M^2}{3\alpha_M^2}$ for notational simplicity. The output vector $\mathbf{v} \triangleq [v_1, \dots, v_{N_R}]^T \in \mathbb{M}^{N_R}$ from the feedback section is finally filtered by the forward filter $\mathbf{F}^H \in \mathbb{C}^{N_T \times N_R}$ to get the transmit signal \mathbf{x} . The elements of \mathbf{v} are assumed to be mutually uncorrelated: $\Phi_{vv} \triangleq \mathbb{E}[\mathbf{v}\mathbf{v}^H] = \text{diag}(\sigma_{v_1}^2, \dots, \sigma_{v_{N_R}}^2) \in \mathbb{R}^{N_R \times N_R}$. Two constraints have to be satisfied by the precoding filters. The first one is to limit the total transmit power to a certain value E_s . The second constraint is imposed on the backward filter ($\mathbf{B}^H - \mathbf{I}$) which must have a strict triangular structure for the causality of the feedback process. The complete precoding procedure is concisely summarized in Table V.

The received signal y_j at the j th antenna is multiplied with the automatic gain control $1/\beta \in \mathbb{R}_+$ which would be determined by pilot signals in practice, then the modulo operator $M(\cdot)$ is applied to get rid of the respective effect of $M(\cdot)$ at the transmitter. The quantizer $Q(\cdot)$ generates the estimate \hat{u}_j .

Our goal is to jointly optimize the backward and forward filters. In order to formulate the joint optimization using only a linear system, the nonlinear modulo operator in Fig. 6 is interpreted by the linear representation as shown in Fig. 8. We introduce the signals $\mathbf{a} \triangleq [a_1, \dots, a_{N_R}]^T \in \mathbb{C}^{N_R}$ and $\mathbf{d} \triangleq [d_1, \dots, d_{N_R}]^T \in \mathbb{C}^{N_R}$ which force \mathbf{v} to be in the set \mathbb{M}^{N_R} . The real and imaginary parts of \mathbf{a} are integer multiples of $2M/\alpha_M$ as can be understood with (24). The signal \mathbf{v} can be written as $\mathbf{v} = \mathbf{P}\mathbf{d} - (\mathbf{B}^H - \mathbf{I})\mathbf{v}$ [cf. Fig. 8], which we solve for \mathbf{d} yielding $\mathbf{d} = \mathbf{P}^T \mathbf{B}^H \mathbf{v}$ while the estimated signal at the receiver reads as

$\hat{\mathbf{d}} = \beta^{-1} \mathbf{H} \mathbf{F}^H \mathbf{v} + \beta^{-1} \mathbf{n}$. By defining the error signal $\boldsymbol{\varepsilon} \triangleq \hat{\mathbf{d}} - \mathbf{d}$, the MSE φ is written as

$$\varphi \triangleq \mathbb{E}[\boldsymbol{\varepsilon}^H \boldsymbol{\varepsilon}] = \text{tr}(\boldsymbol{\Phi}_{\boldsymbol{\varepsilon}\boldsymbol{\varepsilon}}) \quad \text{where} \quad \boldsymbol{\Phi}_{\boldsymbol{\varepsilon}\boldsymbol{\varepsilon}} \triangleq \mathbb{E}[\boldsymbol{\varepsilon} \boldsymbol{\varepsilon}^H]. \quad (25)$$

This is the cost function to be minimized. With the two constraints of the transmit power and the strict lower triangular structure of the backward filter, the optimization problem is stated as

$$\begin{aligned} \{\mathbf{F}_{\text{opt}}, \mathbf{B}_{\text{opt}}, \beta_{\text{opt}}\} &= \arg \min_{\{\mathbf{F}, \mathbf{B}, \beta\}} \varphi \\ \text{s.t. : } \mathbb{E}[\|\mathbf{x}\|_2^2] &= \text{tr}(\mathbf{F}^H \boldsymbol{\Phi}_{vv} \mathbf{F}) = E_s \quad \text{and} \\ \mathbf{S}_j (\mathbf{B}^H - \mathbf{I}_{N_R}) \mathbf{e}_j &= \mathbf{0}_{j \times 1} \quad \text{for } j = 1, \dots, N_R \end{aligned} \quad (26)$$

where the selection matrix \mathbf{S}_j is now defined as $\mathbf{S}_j \triangleq [\mathbf{I}_j \mathbf{0}_{j \times N_R - j}] \in \{0, 1\}^{j \times N_R}$. Note that the constraint for the strict lower triangular structure is defined for every column of the backward filter so that its upper triangular part must be zero. This optimization problem can be solved using Lagrangian multipliers [29] and we get the solution for the forward and backward filters (see Appendix II)

$$\begin{aligned} \mathbf{F}_{\text{opt}}^H &= \beta_{\text{opt}} \sum_{j=1}^{N_R} \mathbf{H}^H \mathbf{P}^T \mathbf{S}_j^T \left(\mathbf{S}_j \mathbf{P} \boldsymbol{\Phi} \mathbf{P}^T \mathbf{S}_j^T \right)^{-1} \mathbf{S}_j \mathbf{e}_j \mathbf{e}_j^T \\ \mathbf{B}_{\text{opt}}^H &= \sum_{j=1}^{N_R} \mathbf{P} \boldsymbol{\Phi} \mathbf{P}^T \mathbf{S}_j^T \left(\mathbf{S}_j \mathbf{P} \boldsymbol{\Phi} \mathbf{P}^T \mathbf{S}_j^T \right)^{-1} \mathbf{S}_j \mathbf{e}_j \mathbf{e}_j^T \end{aligned} \quad (27)$$

where we defined

$$\gamma \triangleq \frac{E_s}{\text{tr}(\boldsymbol{\Phi}_{nn})} \quad \text{and} \quad \boldsymbol{\Phi} \triangleq \mathbf{H} \mathbf{H}^H + \gamma^{-1} \mathbf{I}_{N_R}. \quad (28)$$

The optimum scalar $\beta_{\text{opt}} \in \mathbb{R}_+$ can be easily calculated to satisfy the transmit power constraint in (26). As we can see from (27), the filters are determined column by column, each of which requires one matrix inverse resulting in the total complexity order of $O(N_R^4)$. That becomes quite complex for large N_R . Readers are referred to [24] for the complete description of the algorithm based on the above solution.

A. Ordering Strategy for Precoding

Before we present our computationally efficient solutions, let us discuss the ordering strategy for precoding. We consider a simple example of two data streams illustrated in Fig. 9 to discuss the difference. For DFE, let us assume that x_1 is detected first, then x_2 . There is one interferer x_2 when detecting x_1 while after its detection and cancellation, x_2 is interference free and easier to detect. This is true if there is no error propagation from x_1 . Therefore, to reduce the risk of the error propagation, the ordering strategy for V-BLAST is known as “best first,” i.e., always choosing the best data stream at every detection stage.

For THP, we assume that u_1 is precoded first, then u_2 in Fig. 9. There is no interferer when precoding u_1 , or in other words, the precoder can neglect the other data stream u_2 since the precoded signal of u_1 , which will interfere with u_2 , can be cancelled out by the feedback processing. After precoding u_1 and its cancellation of the interference to u_2 , precoding u_2 is the more difficult task. That is because u_2 is a potential interferer

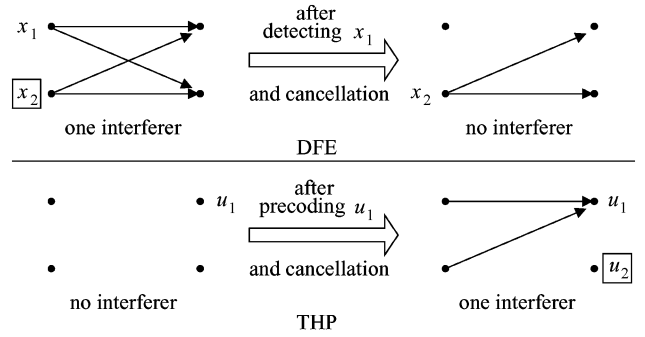


Fig. 9. Difference between successive detection and precoding. The signal shown in the box is the interferer. For DFE, detecting x_2 is easier than x_1 after x_1 is detected and cancelled out. For THP, precoding u_2 is more difficult than u_1 since it must avoid interfering the already precoded u_1 .

to u_1 , and, thus, it is necessary to avoid interfering the already precoded u_1 .

To generalize, as the successive precoding process proceeds, we should avoid interfering all the already precoded data streams. The interference to the data streams, which are to be precoded later, can be cancelled out by the feedback process. From the filter optimization point of view, the data stream to be precoded later, has to take into account more constraints and it has less degrees of freedom. This is exactly the opposite situation of DFE. Therefore, for THP we start choosing the best data stream which is to be precoded last, i.e., we apply a “best last” rule to find the precoding ordering in order to give the later precoded data stream a better chance. This ordering direction is reported in [24] and also known from the MSE uplink-downlink duality, e.g., [33] and [34]. We observed by means of computer simulations that this ordering strategy performs close to the globally optimum solution achieving the minimum bit errors among all possible orderings. Thereby, we refer to this ordering “optimum” in the sequel.

B. Optimum MMSE THP Applying Cholesky Factorization With Symmetric Permutation

This section presents our computationally efficient optimum algorithm. We show that the results in (27) can be greatly simplified by

$$\mathbf{P} \boldsymbol{\Phi}^{-1} \mathbf{P}^T = \mathbf{L}^H \mathbf{D} \mathbf{L} \quad (29)$$

where $\mathbf{L} \in \mathbb{C}^{N_R \times N_R}$ and $\mathbf{D} \triangleq \text{diag}(d_1, \dots, d_{N_R}) \in \mathbb{R}^{N_R \times N_R}$ are respectively a unit lower triangular matrix and a diagonal matrix. The Cholesky factorization with symmetric permutation of (29) can be computed, since $\boldsymbol{\Phi}$ is Hermitian and also positive definite. Later in this section we will also show that the factorization of (29) leads to the optimum precoding ordering strategy which we discussed in the previous section. With (29), the forward and backward filters in (27) reduce to (see Appendix II)

$$\mathbf{F}_{\text{opt}}^H = \beta_{\text{opt}} \mathbf{H}^H \mathbf{P}^T \mathbf{L}^H \mathbf{D} \quad \text{and} \quad \mathbf{B}_{\text{opt}}^H = \mathbf{L}^{-1}. \quad (30)$$

This is a significant computational complexity reduction compared to (27). Instead of N_R times matrix inversions, we compute $\boldsymbol{\Phi}^{-1}$, its factorization in (29), and the inversion of the triangular matrix \mathbf{L} . The proposed algorithm computing the filters is

TABLE VI

CALCULATION OF THP FILTERS WITH *OPTIMUM* PRECODING ORDERING
(DIFFERENCE FROM *SUBOPTIMUM* DFE FILTER COMPUTATION IN TABLE III)

$$\begin{array}{l}
1: \Phi^{-1} = (\mathbf{H}\mathbf{H}^H + \gamma^{-1}\mathbf{I}_{N_R})^{-1}, \mathbf{P} = \mathbf{I}_{N_R}, \mathbf{D} = \mathbf{0}_{N_R} \\
\Phi_{\varepsilon\varepsilon}^{-1} \mapsto \Phi^{-1}, N_T \mapsto N_R, i \leftrightarrow j \\
2: \text{for } j = N_R, \dots, 1 \\
3: q = \underset{q'=1, \dots, j}{\operatorname{argmin}} \sigma_{v_q}^2 \Phi^{-1}(q', q') \\
11: \mathbf{B}^H = \mathbf{L}^{-1}, \mathbf{F}^H = \mathbf{H}^H \mathbf{P}^T \mathbf{L}^H \mathbf{D} \\
\chi = \|\mathbf{F}^H(:, 1)\|_2^2 + \sigma_v^2 \|\mathbf{F}^H(:, 2:N_R)\|_F^2, \\
\beta = \sqrt{E_s/\chi}, \mathbf{F}^H = \beta \mathbf{F}^H
\end{array}$$

summarized as a pseudo code in Table VI. The precoding procedure using the computed filters and ordering can be found in Table V.

Now, we are going to show that the algorithm in Table VI finds the optimum ordering. Using the solution in (30), it can be shown that the MSE in (25) can be rewritten as (see Appendix II)

$$\varphi = \gamma^{-1} \operatorname{tr}(\mathbf{D}\Phi_{vv}) = \gamma^{-1} \sum_{j=1}^{N_R} \sigma_{v_j}^2 d_j. \quad (31)$$

When we successively choose the precoding ordering so as to minimize φ , the optimum strategy is to start choosing the data stream which will be precoded last (see Section IV-A). Thus, we can write

$$k_j = \underset{k \in \{k_{j+1}, \dots, k_{N_R}\}}{\operatorname{argmin}} \sigma_{v_k}^2 d_k \quad (32)$$

where γ^{-1} in (31) is independent of the ordering [cf. (20) for MMSE V-BLAST]. It can be observed from Table VI that the algorithm determines the precoding ordering based on (32).

C. Suboptimum MMSE THP Applying Cholesky Factorization With Symmetric Permutation

The proposed optimum ordered Cholesky approach described in the previous section requires the matrix inverse of Φ . To avoid this inversion, we can also compute the following factorization:

$$\mathbf{P}\Phi\mathbf{P}^T = \mathbf{L}'\mathbf{D}'\mathbf{L}'^H \quad (33)$$

where $\mathbf{L}' \in \mathbb{C}^{N_R \times N_R}$ and $\mathbf{D}' \triangleq \operatorname{diag}(d'_1, \dots, d'_{N_R}) \in \mathbb{R}^{N_R \times N_R}$ are a unit lower triangular matrix and a diagonal matrix, respectively. Since we can rewrite (33) as $\mathbf{P}\Phi^{-1}\mathbf{P}^T = \mathbf{L}'^{-H}\mathbf{D}'^{-1}\mathbf{L}'^{-1}$ [cf. (29)] and also because the inverse of unit triangular matrix is again unit lower triangular, we can reuse the result of the optimum solution in (30). We replace \mathbf{L} and \mathbf{D} in (30) by \mathbf{L}'^{-1} and \mathbf{D}'^{-1} , respectively, to get

$$\mathbf{F}_{\text{subopt}}^H = \beta_{\text{subopt}} \mathbf{H}^H \mathbf{P}^T \mathbf{L}'^{-H} \mathbf{D}'^{-1} \quad \text{and} \quad \mathbf{B}_{\text{subopt}}^H = \mathbf{L}'. \quad (34)$$

The algorithm for computing the filters is summarized as a pseudo code in Table VII.

To discuss why this is the suboptimum solution, we start with the computation of the MSE. The MSE can be obtained from (31) by substituting d_j with d'_j as follows:

TABLE VII

CALCULATION OF THP FILTERS WITH *SUBOPTIMUM* PRECODING ORDERING
(DIFFERENCE FROM *OPTIMUM* DFE FILTER COMPUTATION IN TABLE II)

$$\begin{array}{l}
1: \Phi = \mathbf{H}\mathbf{H}^H + \gamma^{-1}\mathbf{I}_{N_R}, \mathbf{P} = \mathbf{I}_{N_R}, \mathbf{D} = \mathbf{0}_{N_R} \\
\Phi_{\varepsilon\varepsilon} \mapsto \Phi, N_T \mapsto N_R, i \leftrightarrow j \\
2: \text{for } j = 1, \dots, N_R \\
3: q = \underset{q'=j, \dots, N_R}{\operatorname{argmin}} \Phi(q', q') / \sigma_{v_q}^2 \\
11: \mathbf{B}^H = \mathbf{L}, \mathbf{F}^H = \mathbf{H}^H \mathbf{P}^T \mathbf{L}^{-H} \mathbf{D}^{-1} \\
\chi = \|\mathbf{F}^H(:, 1)\|_2^2 + \sigma_v^2 \|\mathbf{F}^H(:, 2:N_R)\|_F^2, \\
\beta = \sqrt{E_s/\chi}, \mathbf{F}^H = \beta \mathbf{F}^H
\end{array}$$

$\varphi = \gamma^{-1} \sum_{j=1}^{N_R} \sigma_{v_j}^2 d'_j$. This result suggests to choose the data stream, which has the minimum value of $\sigma_{v_j}^2 d'_j$, at every stage of the successive processing. However, we observe from Table VII that we must start choosing the first precoded data stream. That is the reverse direction to the optimum strategy as we discussed in Section IV-A. Therefore, we choose the worst data stream at every optimization step so that it can have a better condition or in other words, less interference. This condition can be written as

$$k_j = \underset{k \in \{k_1, \dots, k_{j-1}\}}{\operatorname{argmin}} d'_k / \sigma_{v_k}^2$$

which can be seen from Table VII. Since the optimization direction is opposite to the desired strategy, this algorithm does not always lead to the optimum ordering.

D. Complexity Analysis

We compare the computational complexity of the proposed algorithms with that of the original THP in [24]. The proposed algorithm for THP is similar to that for DFE. The major difference from the DFE solution is that we need to compute the forward filter \mathbf{F}^H explicitly in order to determine the normalization factor satisfying the transmit power constraint. The results are summarized in Table VIII which shows only the terms above the second order. If $N_T = N_R$, then the speedup of the proposed optimum solution over the original THP in the number of both multiplications and additions is roughly $1.64N_R + 3.80$. Our suboptimum solution is faster by a factor of roughly $2.25N_R + 5.25$ for both multiplications and additions. Note that the complexity of our suboptimum solution for THP is roughly regarded as that of a simple linear transmit filter (e.g., [25]).

E. Numerical Results

Computer simulations are performed to evaluate the uncoded BER performance over E_b/N_0 [cf. (2)]. In the following, we assume a white input signal and noise, i.e., $E[\mathbf{u}\mathbf{u}^H] = \mathbf{I}_{N_R}$ and $\Phi_{nn} = \sigma_n^2 \mathbf{I}_{N_R}$. The frame length of 1000 information bits are QPSK modulated ($M = 2$). The channel is quasi static and assumed to be perfectly known at the transmitter.

Fig. 10 shows the performance of a system with $N_T = N_R = 4$ antennas both at the transmitter and the receiver. The impact of the ordering optimization can be observed. The performance of the MMSE linear filter is also plotted for comparison. Significant gain of the nonlinear THP against the linear filter can be seen. Our optimum algorithm achieves the same performance as the reference scheme in [24], but the complexity is drastically

TABLE VIII
COMPLEXITY COMPARISON OF PROPOSED PRECODING SCHEMES

	THP in [24]	optimum Cholesky	suboptimum Cholesky
multiplications	$N_R^2(3N_R^2 + 6N_R + N_T)$	$\frac{1}{6}N_R^2(5N_R + 6N_T)$	$\frac{1}{6}N_R^2(2N_R + 6N_T)$
additions	$N_R^2(3N_R^2 + 6N_R + N_T)$	$\frac{1}{6}N_R^2(5N_R + 6N_T)$	$\frac{1}{6}N_R^2(2N_R + 6N_T)$

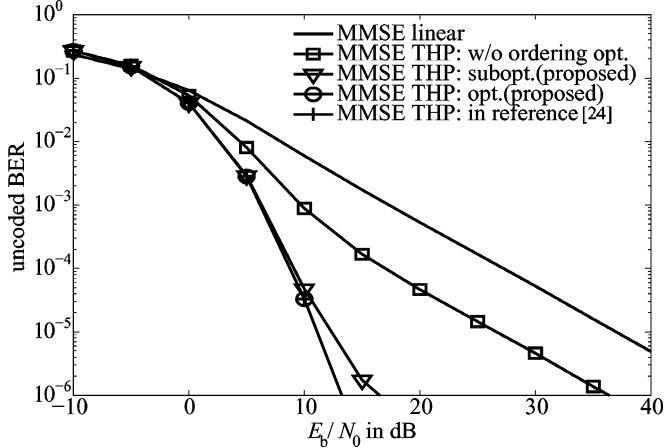


Fig. 10. Uncoded BER performance of a system with $N_T = N_R = 4$ antennas.

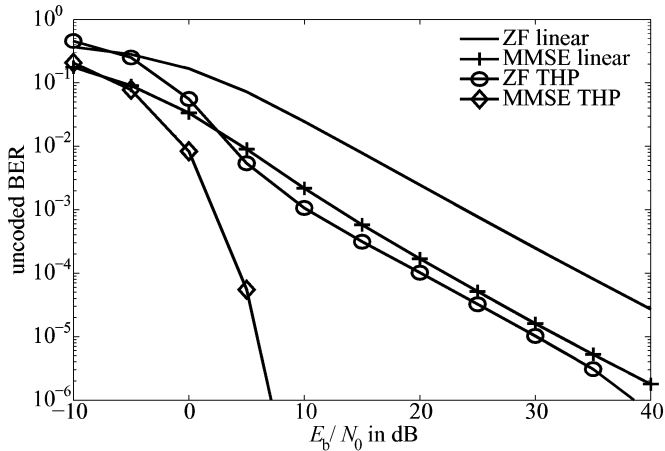


Fig. 11. Uncoded BER performance of a system with $N_T = N_R = 8$ antennas.

reduced. Our suboptimum algorithm shows slight performance degradation in the low uncoded BER region, but no performance degradation in a practical operating point, e.g., uncoded BER of 10^{-2} . We observed that the performance loss due to the suboptimality of the ordering in a wide range of the number of antennas for $N_T = N_R$ is below 0.03 dB at an uncoded BER of 10^{-2} !

Fig. 11 compares the performance of different transmission schemes for a system with $N_T = N_R = 8$ antennas. We conclude that it is possible to obtain the large performance gain against simple linear processing without complexity overhead. The THP approach requires a modulo operation, but its complexity is of minor impact on the total complexity.

V. COMPARISON BETWEEN DFE AND THP

We have shown through the preceding sections that both successive detection and precoding schemes share many ideas in

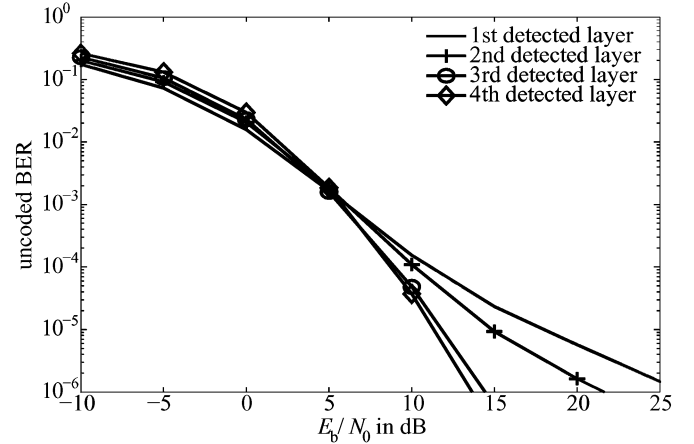


Fig. 12. Performance of *genie* MMSE DFE (V-BLAST) for a system with $N_T = N_R = 4$ antennas. The uncoded BER is plotted for each of the four layers in the order of detection.

common. In this section, we discuss some differences between these schemes. The performance demonstrated in the preceding sections is averaged over all layers and the performance of individual layers is invisible. Contrary, we investigate the performance of individual layers and discuss the impact of the ordering for both schemes in this section.

V-BLAST suffers from error propagation while THP does not. For the purpose of the comparison, we investigate the *genie* detector for V-BLAST. This means that we perform the real interference suppression and detection for each layer, but for subsequent layers we assume ideal detection of the signals of preceding layers [6]. In [6], the authors have demonstrated the pure improvement of the diversity level for the case of no ordering optimization. We illustrate in Fig. 12 the performance including the optimized detection ordering for a system with $N_T = N_R = 4$ antennas. For high SNR, the improvement of the diversity level can be observed as reported in [6] due to the increased degrees of freedom for the layers detected later. However, the performance of layers is reversed for low SNR. To understand this behavior of V-BLAST in the low SNR region, let us consider a white input signal and AWGN noise, i.e., $\Phi_{xx} = \mathbf{I}_{N_T}$ and $\Phi_{nn} = \sigma_n^2 \mathbf{I}_{N_R}$, where we assume $E[|x_i|^2] = 1, \forall i$, without loss of generality. It is well known that the MMSE filter can be approximated as the matched filter for low SNR, that is³ $\mathbf{F}^H \approx \mathbf{H}^H / \sigma_n^2$. Then, the estimates from the filter can be expressed as $\hat{\mathbf{x}} = (1/\sigma_n^2) \mathbf{H}^H \mathbf{H} \mathbf{x} + (1/\sigma_n^2) \mathbf{H}^H \mathbf{n}$. Also, the estimate of the k_1 th layer at the first detection stage reads as

$$\hat{x}_{k_1} = \frac{1}{\sigma_n^2} \|\mathbf{h}_{k_1}\|_2^2 x_{k_1} + \frac{1}{\sigma_n^2} \sum_{j \neq k_1} \mathbf{h}_{k_1}^H \mathbf{h}_j x_j + \frac{1}{\sigma_n^2} \mathbf{h}_{k_1}^H \mathbf{n}$$

³See also (6), with the white input and noise assumption, and for very large σ_n^2 .

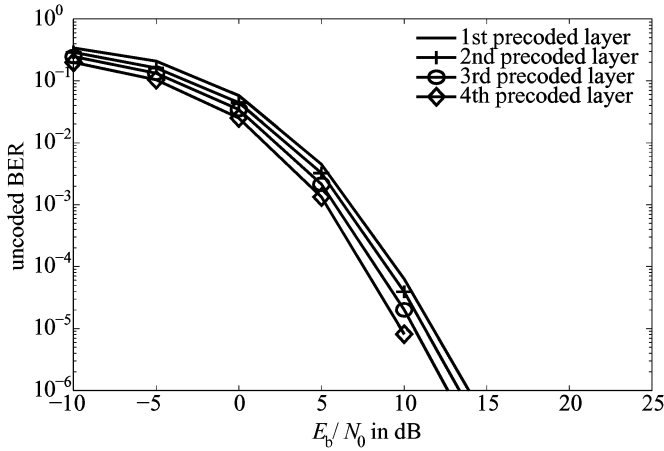


Fig. 13. Performance of MMSE THP for a system with $N_T = N_R = 4$ antennas. The uncoded BER is plotted for each of the four layers in the order of precoding.

where \mathbf{h}_{k_1} denotes the k_1 th column of \mathbf{H} . Since the channel inputs are assumed to be mutually uncorrelated, the *signal to noise plus interference ratio* (SINR) of the k_1 th layer can be written as

$$\frac{\|\mathbf{h}_{k_1}\|_2^4}{\sum_{j \neq k_1} |\mathbf{h}_{k_1}^H \mathbf{h}_j|^2 + \sigma_n^2 \|\mathbf{h}_{k_1}\|_2^2} \approx \frac{\|\mathbf{h}_{k_1}\|_2^2}{\sigma_n^2} \quad \text{for large } \sigma_n^2.$$

This means that the noise is the major factor for the SINR degradation while the interference from the other layers is less significant. The interference from the other layers is reduced by the successive detection. After $i - 1$ layers are detected, the interference from the other layers to the k_i th layer for the updated system can be written as $\sum_{j \notin \{k_1, \dots, k_i\}} |\mathbf{h}_{k_i}^H \mathbf{h}_j|^2$, which is a rather small improvement in the very noisy environment. Also, recall that V-BLAST applies the “best first” rule to choose the best layer at each detection stage. Therefore, the earlier chosen layers perform better than the succeeding layers which take small benefits of interference reduction in the noisy environment. The overall performance of V-BLAST is limited by the worst layer even for the genie detector since there is no power control at the transmitter. For the nongenie detector, the performance is further limited by the error propagation.

Fig. 13 shows the performance of each layer for MMSE THP. Remember that THP applies the “best last” rule to choose the best layer starting from the one precoded last. It can be observed that the last precoded layer successfully takes profit although it has the largest number of constraints (to avoid interference to all the other layers which are already precoded). Furthermore, we can observe that all the layers perform similar, and, thus, the overall performance is not limited by a particular layer. This naturally means that the transmit power is implicitly controlled so as to achieve similar performance for all layers on average.

VI. SUMMARY

We introduced a new common framework for successive detection and precoding of spatially multiplexed data streams over MIMO channels. We illustrated that both schemes could be seen in the view of a system comprising forward and

backward block filters where the latter has a strict triangular structure for the causality of the feedback process. Based on the system model, we strictly derived the optimum forward and backward filters by solving the constrained optimization problem in MMSE sense. The direct solution requires rather high complexity of computing multiple matrix inversions. We proposed to explicitly include the ordering of successive processing into the system model using a permutation matrix. That naturally leads us to apply Cholesky factorization with symmetric permutation to the solution from the constrained optimization problem. The factorization greatly simplifies the solution and reduces the complexity drastically. Since the proposed algorithms require to compute only a triangular part of matrices due to their symmetric nature, that also contributes to the complexity reduction. This framework also led us to suboptimum solutions which show slight performance degradation, but with the complexity roughly equivalent to that of simple linear filters. We concluded that the large performance advantage of nonlinear successive detection and precoding against linear filters is possible without complexity overhead. Finally, we compared the detection and precoding schemes by investigating the performance of individual layers.

APPENDIX I DERIVATION OF MMSE DFE

From (10), the Lagrangian function can be written as

$$\mathcal{L} \triangleq \varphi_p - 2\text{Re} \left\{ \sum_{i=1}^{N_T} \text{tr} \left(\mathbf{S}_i^T \boldsymbol{\mu}_i \mathbf{e}_i^T \mathbf{B}^H \right) - \mathbf{e}_i^T \mathbf{S}_i^T \boldsymbol{\mu}_i \right\} \quad (35)$$

where $\boldsymbol{\mu}_i \in \mathbb{C}^{N_T - i + 1}$, $i = 1, \dots, N_T$, are Lagrangian multipliers. Using (8), we compute the error covariance matrix as

$$\boldsymbol{\Phi}_{\varepsilon\varepsilon}^{(p)} = \mathbf{B}^H \mathbf{P} \boldsymbol{\Phi}_{xx} \mathbf{P}^T \mathbf{B} - \mathbf{F}^H \boldsymbol{\Phi}_{xy}^H \mathbf{P}^T \mathbf{B} - \mathbf{B}^H \mathbf{P} \boldsymbol{\Phi}_{xy} \mathbf{F} + \mathbf{F}^H \boldsymbol{\Phi}_{yy} \mathbf{F}. \quad (36)$$

With (9), (35), and (36), we solve $\partial \mathcal{L} / \partial \mathbf{F}^H = \mathbf{0}$ for \mathbf{F}^H to get

$$\mathbf{F}^H = \mathbf{B}^H \mathbf{P} \boldsymbol{\Phi}_{xy} \boldsymbol{\Phi}_{yy}^{-1} = \mathbf{B}^H \mathbf{P} \boldsymbol{\Phi}_{\varepsilon\varepsilon} \mathbf{H}^H \boldsymbol{\Phi}_{nn}^{-1} \quad (37)$$

where the last equality can be understood by comparing (4) and (6), i.e., $\boldsymbol{\Phi}_{xy} \boldsymbol{\Phi}_{yy}^{-1} = \boldsymbol{\Phi}_{\varepsilon\varepsilon} \mathbf{H}^H \boldsymbol{\Phi}_{nn}^{-1}$. By setting $\partial \mathcal{L} / \partial \mathbf{B}^H = \mathbf{0}$ and using the first equality in (37), we get

$$\mathbf{B}^H \mathbf{P} \left(\underbrace{\boldsymbol{\Phi}_{xx} - \boldsymbol{\Phi}_{xy} \boldsymbol{\Phi}_{yy}^{-1} \boldsymbol{\Phi}_{xy}^H}_{=\boldsymbol{\Phi}_{\varepsilon\varepsilon}} \right) \mathbf{P}^T = \sum_{i=1}^{N_T} \mathbf{e}_i \boldsymbol{\mu}_i^H \mathbf{S}_i.$$

Solving this equation for \mathbf{B}^H gives

$$\mathbf{B}^H = \left(\sum_{i=1}^{N_T} \mathbf{e}_i \boldsymbol{\mu}_i^H \mathbf{S}_i \right) \mathbf{P} \boldsymbol{\Phi}_{\varepsilon\varepsilon}^{-1} \mathbf{P}^T. \quad (38)$$

We plug this result into the constraint in (10) to get

$$\mathbf{e}_i^T \left(\left(\sum_{j=1}^{N_T} \mathbf{e}_j \boldsymbol{\mu}_j^H \mathbf{S}_j \right) \mathbf{P} \boldsymbol{\Phi}_{\varepsilon\varepsilon}^{-1} \mathbf{P}^T - \mathbf{I} \right) \mathbf{S}_i^T = \mathbf{0}_{N_T - i + 1 \times 1}^T. \quad (39)$$

Since

$$\mathbf{e}_i^\top \mathbf{e}_j = \begin{cases} 1, & \text{for } i = j \\ 0, & \text{otherwise} \end{cases} \quad (40)$$

holds, (39) can be simplified and we solve for $\boldsymbol{\mu}_i^H$:

$$\boldsymbol{\mu}_i^H = \mathbf{e}_i^\top \mathbf{S}_i^\top \left(\mathbf{S}_i \mathbf{P} \boldsymbol{\Phi}_{\varepsilon\varepsilon}^{-1} \mathbf{P}^\top \mathbf{S}_i^\top \right)^{-1}. \quad (41)$$

From (37), (38), and (41), we get the solution for the forward and backward filters in (12).

Now we show that the MSE in (9) can be simplified to (13). Using (37), the error covariance matrix in (36) can be simplified to [see also (5)]

$$\boldsymbol{\Phi}_{\varepsilon\varepsilon}^{(p)} = \mathbf{B}^H \mathbf{P} \boldsymbol{\Phi}_{\varepsilon\varepsilon} \mathbf{P}^\top \mathbf{B}. \quad (42)$$

With (12), it can be rewritten as

$$\boldsymbol{\Phi}_{\varepsilon\varepsilon}^{(p)} = \sum_{i=1}^{N_T} \sum_{j=1}^{N_T} \mathbf{e}_i \mathbf{e}_i^\top \mathbf{S}_i^\top \boldsymbol{\Psi}_i^{-1} \mathbf{S}_i \mathbf{P} \boldsymbol{\Phi}_{\varepsilon\varepsilon}^{-1} \mathbf{P}^\top \mathbf{S}_j^\top \boldsymbol{\Psi}_j^{-1} \mathbf{S}_j \mathbf{e}_j \mathbf{e}_j^\top \quad (43)$$

where we defined

$$\boldsymbol{\Psi}_i \triangleq \mathbf{S}_i \mathbf{P} \boldsymbol{\Phi}_{\varepsilon\varepsilon}^{-1} \mathbf{P}^\top \mathbf{S}_i^\top. \quad (44)$$

Using (43) and $\text{tr}(\mathbf{A}\mathbf{B}) = \text{tr}(\mathbf{B}\mathbf{A})$, (9) can be computed as follows:

$$\begin{aligned} \varphi_p &= \sum_{i=1}^{N_T} \sum_{j=1}^{N_T} \text{tr} \left(\mathbf{e}_j^\top \mathbf{e}_i \mathbf{e}_i^\top \mathbf{S}_i^\top \boldsymbol{\Psi}_i^{-1} \mathbf{S}_i \mathbf{P} \boldsymbol{\Phi}_{\varepsilon\varepsilon}^{-1} \mathbf{P}^\top \mathbf{S}_j^\top \boldsymbol{\Psi}_j^{-1} \mathbf{S}_j \mathbf{e}_j \right) \\ &= \sum_{i=1}^{N_T} \mathbf{e}_i^\top \mathbf{S}_i^\top \boldsymbol{\Psi}_i^{-1} \mathbf{S}_i \mathbf{P} \boldsymbol{\Phi}_{\varepsilon\varepsilon}^{-1} \mathbf{P}^\top \mathbf{S}_i^\top \boldsymbol{\Psi}_i^{-1} \mathbf{S}_i \mathbf{e}_i \\ &= \sum_{i=1}^{N_T} \mathbf{e}_i^\top \mathbf{S}_i^\top \boldsymbol{\Psi}_i^{-1} \mathbf{S}_i \mathbf{e}_i. \end{aligned} \quad (45)$$

Before we further proceed, let us introduce the following lemma.

Lemma 1: $(\mathbf{S}_i \mathbf{A} \mathbf{S}_i^\top)^{-1} = \mathbf{S}_i (\mathbf{S}_i^\top \mathbf{S}_i \mathbf{A} \mathbf{S}_i^\top \mathbf{S}_i)^\dagger \mathbf{S}_i^\top$ holds for $\mathbf{A} \in \mathbb{C}^{N_T \times N_T}$ if $\mathbf{S}_i \mathbf{A} \mathbf{S}_i^\top$ is invertible. $(\cdot)^\dagger$ denotes pseudo inverse.

Proof: Let us define a partition of \mathbf{A} as

$$\mathbf{A} \triangleq \begin{bmatrix} \mathbf{A}_{1,1} & \mathbf{A}_{1,2} \\ \mathbf{A}_{2,1} & \mathbf{A}_{2,2} \end{bmatrix} \quad (46)$$

where the dimensions of the square matrices of $\mathbf{A}_{1,1}$ and $\mathbf{A}_{2,2}$ are, respectively, $i-1$ and N_T-i+1 . Then, the left-hand side of Lemma 1 is expressed as

$$\left(\mathbf{S}_i \mathbf{A} \mathbf{S}_i^\top \right)^{-1} = \mathbf{A}_{2,2}^{-1}. \quad (47)$$

For the right-hand side, we compute

$$\left(\mathbf{S}_i^\top \mathbf{S}_i \mathbf{A} \mathbf{S}_i^\top \mathbf{S}_i \right)^\dagger = \begin{bmatrix} \mathbf{0} & \mathbf{0} \\ \mathbf{0} & \mathbf{A}_{2,2} \end{bmatrix}^\dagger = \begin{bmatrix} \mathbf{0} & \mathbf{0} \\ \mathbf{0} & \mathbf{A}_{2,2}^{-1} \end{bmatrix}.$$

Therefore, $\mathbf{S}_i (\mathbf{S}_i^\top \mathbf{S}_i \mathbf{A} \mathbf{S}_i^\top \mathbf{S}_i)^\dagger \mathbf{S}_i^\top = \mathbf{A}_{2,2}^{-1}$ which is equivalent to the left-hand side. \blacksquare

Using Lemma 1 and with (44), (45) can be computed as

$$\begin{aligned} \varphi_p &= \sum_{i=1}^{N_T} \mathbf{e}_i^\top \mathbf{S}_i^\top \left(\mathbf{S}_i \mathbf{P} \boldsymbol{\Phi}_{\varepsilon\varepsilon}^{-1} \mathbf{P}^\top \mathbf{S}_i^\top \right)^{-1} \mathbf{S}_i \mathbf{e}_i \\ &= \sum_{i=1}^{N_T} \mathbf{e}_i^\top \mathbf{S}_i^\top \mathbf{S}_i \mathbf{P} \left(\mathbf{P}^\top \mathbf{S}_i^\top \mathbf{S}_i \mathbf{P} \boldsymbol{\Phi}_{\varepsilon\varepsilon}^{-1} \mathbf{P}^\top \mathbf{S}_i^\top \mathbf{S}_i \mathbf{P} \right)^\dagger \\ &\quad \times \mathbf{P}^\top \mathbf{S}_i^\top \mathbf{S}_i \mathbf{e}_i. \end{aligned} \quad (48)$$

From the definition in (11), it is easy to see that the following equality holds:

$$\mathbf{S}_i^\top \mathbf{S}_i \mathbf{e}_j = \begin{cases} \mathbf{0}, & j < i \\ \mathbf{e}_j, & j \geq i \end{cases} \quad (49)$$

and, therefore

$$\mathbf{S}_i^\top \mathbf{S}_i \mathbf{P} = \mathbf{S}_i^\top \mathbf{S}_i \sum_{j=1}^{N_T} \mathbf{e}_j \mathbf{e}_{k_j}^\top = \sum_{j=i}^{N_T} \mathbf{e}_j \mathbf{e}_{k_j}^\top.$$

Thus, we get $\mathbf{e}_i^\top \mathbf{S}_i^\top \mathbf{S}_i \mathbf{P} = \mathbf{e}_{k_i}^\top$. Using this result for (48), we finally get (13).

In the following, we show that the factorization in (16) simplifies the solution in (12) and the MSE φ_p in (9). Let us first introduce the following lemmas.

Lemma 2: $\mathbf{S}_i \mathbf{A} \mathbf{A} \mathbf{A}^H \mathbf{S}_i^\top = \mathbf{S}_i \mathbf{A} \mathbf{S}_i^\top \mathbf{S}_i \mathbf{A} \mathbf{S}_i^\top \mathbf{S}_i \mathbf{A}^H \mathbf{S}_i^\top$ holds for a diagonal matrix $\mathbf{A} \in \mathbb{C}^{N_T \times N_T}$ and an upper triangular matrix $\mathbf{A} \in \mathbb{C}^{N_T \times N_T}$.

Proof: We consider $\mathbf{A} = \text{blockdiag}(\mathbf{A}_1, \mathbf{A}_2)$, $\mathbf{A}_1 \in \mathbb{C}^{i-1 \times i-1}$, $\mathbf{A}_2 \in \mathbb{C}^{N_T-i+1 \times N_T-i+1}$, and the partition of \mathbf{A} defined in (46) where $\mathbf{A}_{2,1} = \mathbf{0}$. The both sides of Lemma 2 are computed as $\mathbf{A}_{2,2} \mathbf{A}_2 \mathbf{A}_2^H$ since $\mathbf{S}_i \mathbf{A} = [\mathbf{0}, \mathbf{A}_{2,2}]$, $\mathbf{S}_i \mathbf{A} \mathbf{S}_i^\top = \mathbf{A}_{2,2}$, and $\mathbf{S}_i \mathbf{A} \mathbf{S}_i^\top = \mathbf{A}_2$ hold. \blacksquare

Lemma 3: $(\mathbf{S}_i \mathbf{A} \mathbf{S}_i^\top)^{-1} = \mathbf{S}_i \mathbf{A}^{-1} \mathbf{S}_i^\top$ holds for a full rank triangular matrix $\mathbf{A} \in \mathbb{C}^{N_T \times N_T}$.

Proof: We consider the partition of \mathbf{A} defined in (46). The left-hand side of Lemma 3 is given in (47) while the right-hand side is the inverse of the Schur complement of $\mathbf{A}_{2,2}$ [27, pp. 53] which is written as $(\mathbf{A}_{2,2} - \mathbf{A}_{2,1} \mathbf{A}_{1,1}^{-1} \mathbf{A}_{1,2})^{-1}$. That becomes $\mathbf{A}_{2,2}^{-1}$ since $\mathbf{A}_{1,2} = \mathbf{0}$ or $\mathbf{A}_{2,1} = \mathbf{0}$ holds. \blacksquare

With (16), Lemma 2, and Lemma 3, (41) can be rewritten as

$$\begin{aligned} \boldsymbol{\mu}_i^H &= \mathbf{e}_i^\top \mathbf{S}_i^\top \left(\mathbf{S}_i \mathbf{L}^{-H} \mathbf{D}^{-1} \mathbf{L}^{-1} \mathbf{S}_i^\top \right)^{-1} \\ &= \mathbf{e}_i^\top \mathbf{S}_i^\top \left(\mathbf{S}_i \mathbf{L}^{-H} \mathbf{S}_i^\top \mathbf{S}_i \mathbf{D}^{-1} \mathbf{S}_i^\top \mathbf{S}_i \mathbf{L}^{-1} \mathbf{S}_i^\top \right)^{-1} \\ &= \mathbf{e}_i^\top \mathbf{S}_i^\top \left(\mathbf{S}_i \mathbf{L} \mathbf{S}_i^\top \right) \left(\mathbf{S}_i \mathbf{D} \mathbf{S}_i^\top \right) \left(\mathbf{S}_i \mathbf{L}^H \mathbf{S}_i^\top \right) \\ &= \mathbf{e}_i^\top \mathbf{D} \mathbf{S}_i^\top \mathbf{S}_i \mathbf{L}^H \mathbf{S}_i^\top. \end{aligned} \quad (50)$$

We applied $\mathbf{e}_i^\top \mathbf{L} \mathbf{S}_i^\top \mathbf{S}_i = \mathbf{e}_i^\top$ which should be clear for the unit lower triangular matrix \mathbf{L} .

Lemma 4: $\mathbf{S}_i^\top \mathbf{S}_i \mathbf{A} \mathbf{S}_i^\top \mathbf{S}_i \mathbf{A}^{-1} = \mathbf{S}_i^\top \mathbf{S}_i$ holds for an upper triangular matrix $\mathbf{A} \in \mathbb{C}^{N_T \times N_T}$.

Proof: Let us consider the partition of \mathbf{A} defined in (46) where $\mathbf{A}_{2,1} = \mathbf{0}$. Then, applying the block matrix inversion lemma yields [27, p. 53]

$$\mathbf{A}^{-1} = \begin{bmatrix} \mathbf{A}_{1,1}^{-1} & -\mathbf{A}_{1,1}^{-1} \mathbf{A}_{1,2} \mathbf{A}_{2,2}^{-1} \\ \mathbf{0} & \mathbf{A}_{2,2}^{-1} \end{bmatrix}.$$

Using this result, we get

$$\mathbf{S}_i^T \mathbf{S}_i \mathbf{A} = \begin{bmatrix} \mathbf{0} & \mathbf{0} \\ \mathbf{0} & \mathbf{A}_{2,2} \end{bmatrix} \quad \text{and} \quad \mathbf{S}_i^T \mathbf{S}_i \mathbf{A}^{-1} = \begin{bmatrix} \mathbf{0} & \mathbf{0} \\ \mathbf{0} & \mathbf{A}_{2,2}^{-1} \end{bmatrix}.$$

Multiplication of these results proves Lemma 4. \blacksquare

Using Lemma 4, (16), (38), and (50) can be computed as follows:

$$\begin{aligned} \mathbf{B}^H &= \sum_{i=1}^{N_T} \mathbf{e}_i \mathbf{e}_i^T \mathbf{D} \left(\mathbf{S}_i^T \mathbf{S}_i \mathbf{L}^H \mathbf{S}_i^T \mathbf{S}_i \mathbf{L}^{-H} \right) \mathbf{D}^{-1} \mathbf{L}^{-1} \\ &= \sum_{i=1}^{N_T} \mathbf{e}_i \mathbf{e}_i^T \mathbf{D} \mathbf{S}_i^T \mathbf{S}_i \mathbf{D}^{-1} \mathbf{L}^{-1} \\ &= \mathbf{L}^{-1}. \end{aligned}$$

With this result and (16), the forward filter in (37) can be also simplified, and we get (17). Similarly, the error covariance in (42) reduces to (18).

APPENDIX II DERIVATION OF MMSE THP

From (26), the Lagrangian function reads as

$$\begin{aligned} \mathcal{L} \triangleq & \varphi - \rho \left(\text{tr}(\mathbf{F}^H \Phi_{vv} \mathbf{F}) - E_s \right) \\ & - 2\text{Re} \left\{ \sum_{j=1}^{N_R} \boldsymbol{\mu}_j^H \mathbf{S}_j \mathbf{B}^H \mathbf{e}_j - \boldsymbol{\mu}_j^H \mathbf{S}_j \mathbf{e}_j \right\} \end{aligned} \quad (51)$$

where $\rho \in \mathbb{R}$ and $\boldsymbol{\mu}_j \in \mathbb{C}^j$, $j = 1, \dots, N_R$, are Lagrangian multipliers. From (25) the error covariance matrix is calculated as

$$\begin{aligned} \Phi_{\varepsilon\varepsilon} = & \beta^{-2} \mathbf{H} \mathbf{F}^H \Phi_{vv} \mathbf{F} \mathbf{H}^H + \mathbf{P}^T \mathbf{B}^H \Phi_{vv} \mathbf{B} \mathbf{P} - \beta^{-1} \mathbf{H} \mathbf{F}^H \Phi_{vv} \mathbf{B} \mathbf{P} \\ & - \beta^{-1} \mathbf{P}^T \mathbf{B}^H \Phi_{vv} \mathbf{F} \mathbf{H}^H + \beta^{-2} \Phi_{nn} \end{aligned} \quad (52)$$

where we assume $\mathbb{E}[\mathbf{v} \mathbf{v}^H] = \mathbf{0}$. From (25), (51), and (52), we solve $\partial \mathcal{L} / \partial \mathbf{F}^H = \mathbf{0}$, then we obtain the following relation:

$$\mathbf{F} \mathbf{H}^H \mathbf{H} - \beta \mathbf{B} \mathbf{P} \mathbf{H} = \rho \beta^2 \mathbf{F} \quad (53)$$

which will be useful shortly after, and we also solve for \mathbf{F}^H to get

$$\begin{aligned} \mathbf{F}^H &= \beta \left(\mathbf{H}^H \mathbf{H} - \rho \beta^2 \mathbf{I}_{N_T} \right)^{-1} \mathbf{H}^H \mathbf{P}^T \mathbf{B}^H \\ &= \beta \mathbf{H}^H \left(\mathbf{H} \mathbf{H}^H - \rho \beta^2 \mathbf{I}_{N_R} \right)^{-1} \mathbf{P}^T \mathbf{B}^H. \end{aligned} \quad (54)$$

The partial derivative of \mathcal{L} with respect to β reads as

$$\begin{aligned} \frac{\partial \mathcal{L}}{\partial \beta} &= -2\beta^{-3} \text{tr}(\mathbf{H} \mathbf{F}^H \Phi_{vv} \mathbf{F} \mathbf{H}^H) \\ &+ 2\beta^{-2} \text{Re} \left\{ \text{tr}(\mathbf{H} \mathbf{F}^H \Phi_{vv} \mathbf{B} \mathbf{P}) \right\} - 2\beta^{-3} \text{tr}(\Phi_{nn}) \\ &= -2\beta^{-3} \text{tr} \left(\mathbf{F}^H \Phi_{vv} (\mathbf{F} \mathbf{H}^H \mathbf{H} - \beta \mathbf{B} \mathbf{P} \mathbf{H}) \right) \\ &- 2\beta^{-3} \text{tr}(\Phi_{nn}) \\ &= -2\beta^{-1} \rho \text{tr}(\mathbf{F}^H \Phi_{vv} \mathbf{F}) - 2\beta^{-3} \text{tr}(\Phi_{nn}) \\ &= -2\beta^{-1} (\rho E_s + \beta^{-2} \text{tr}(\Phi_{nn})) \end{aligned}$$

where we used (53) to get the third equality. Solving $\partial \mathcal{L} / \partial \beta = 0$ gives $\rho \beta^2 = -\gamma^{-1}$ [cf. (28)]. Using this result and (28), (54) can be rewritten as

$$\mathbf{F}^H = \beta \mathbf{H}^H \Phi^{-1} \mathbf{P}^T \mathbf{B}^H. \quad (55)$$

From $\partial \mathcal{L} / \partial \mathbf{B}^H = \mathbf{0}$ and using (55), we get

$$\begin{aligned} \sum_{j=1}^{N_R} \mathbf{S}_j^T \boldsymbol{\mu}_j \mathbf{e}_j^T &= \mathbf{B}^H \Phi_{vv} - \mathbf{P} \mathbf{H} \mathbf{H}^H \Phi^{-1} \mathbf{P}^T \mathbf{B}^H \Phi_{vv} \\ &= \mathbf{P} (\Phi - \mathbf{H} \mathbf{H}^H) \Phi^{-1} \mathbf{P}^T \mathbf{B}^H \Phi_{vv} \\ &= \gamma^{-1} \mathbf{P} \Phi^{-1} \mathbf{P}^T \mathbf{B}^H \Phi_{vv}. \end{aligned}$$

From this result, \mathbf{B}^H can be expressed as

$$\mathbf{B}^H = \sum_{j=1}^{N_R} \frac{\gamma}{\sigma_{v_j}^2} \mathbf{P} \Phi \mathbf{P}^T \mathbf{S}_j^T \boldsymbol{\mu}_j \mathbf{e}_j^T \quad (56)$$

where we used $\Phi_{vv} = \text{diag}(\sigma_{v_1}^2, \dots, \sigma_{v_{N_R}}^2)$ as we have assumed. We plug this result into the second constraint in (26) to get

$$\mathbf{S}_j \left(\sum_{i=1}^{N_R} \frac{\gamma}{\sigma_{v_i}^2} \mathbf{P} \Phi \mathbf{P}^T \mathbf{S}_i^T \boldsymbol{\mu}_i \mathbf{e}_i^T - \mathbf{I}_{N_R} \right) \mathbf{e}_j = \mathbf{0}_{j \times 1}.$$

Due to (40), the summation disappears and we solve for $\boldsymbol{\mu}_j$

$$\boldsymbol{\mu}_j = \gamma^{-1} \sigma_{v_j}^2 \left(\mathbf{S}_j \mathbf{P} \Phi \mathbf{P}^T \mathbf{S}_j^T \right)^{-1} \mathbf{S}_j \mathbf{e}_j. \quad (57)$$

From (55)–(57), we get the solution for the forward and backward filters in (27)

Now we show that (27) can be simplified to (30) using (29). With (29), (57) can be simplified as

$$\begin{aligned} \boldsymbol{\mu}_j &= \gamma^{-1} \sigma_{v_j}^2 \left(\mathbf{S}_j \mathbf{L}^{-1} \mathbf{D}^{-1} \mathbf{L}^{-H} \mathbf{S}_j^T \right)^{-1} \mathbf{S}_j \mathbf{e}_j \\ &= \gamma^{-1} \sigma_{v_j}^2 \left(\mathbf{S}_j \mathbf{L}^{-1} \mathbf{S}_j^T \mathbf{S}_j \mathbf{D}^{-1} \mathbf{S}_j^T \mathbf{S}_j \mathbf{L}^{-H} \mathbf{S}_j^T \right)^{-1} \mathbf{S}_j \mathbf{e}_j \\ &= \gamma^{-1} \sigma_{v_j}^2 \mathbf{S}_j \mathbf{L}^H \mathbf{S}_j^T \mathbf{S}_j \mathbf{D} \mathbf{S}_j^T \mathbf{S}_j \mathbf{L} \mathbf{S}_j^T \mathbf{S}_j \mathbf{e}_j \\ &= \gamma^{-1} \sigma_{v_j}^2 \mathbf{S}_j \mathbf{L}^H \mathbf{S}_j^T \mathbf{S}_j \mathbf{D} \mathbf{e}_j \end{aligned} \quad (58)$$

where we applied $\mathbf{S}_j \boldsymbol{\Lambda} \boldsymbol{\Lambda}^H \mathbf{S}_j^T = \mathbf{S}_j \mathbf{A} \mathbf{S}_j^T \mathbf{S}_j \boldsymbol{\Lambda} \mathbf{S}_j^T \mathbf{S}_j \mathbf{A}^H \mathbf{S}_j^T$ for a diagonal matrix $\boldsymbol{\Lambda} \in \mathbb{C}^{N_R \times N_R}$ and a lower triangular matrix $\mathbf{A} \in \mathbb{C}^{N_R \times N_R}$, and $(\mathbf{S}_j \mathbf{A} \mathbf{S}_j^T)^{-1} = \mathbf{S}_j \mathbf{A}^{-1} \mathbf{S}_j^T$ for a full rank triangular matrix $\mathbf{A} \in \mathbb{C}^{N_R \times N_R}$, which can be easily proved in a similar way as Lemma 2 and Lemma 3, respectively. We also used $\mathbf{S}_j^T \mathbf{S}_j \mathbf{e}_j = \mathbf{e}_j$ and $\mathbf{S}_j^T \mathbf{S}_j \mathbf{L} \mathbf{e}_j = \mathbf{e}_j$ for the unit lower triangular matrix \mathbf{L} . With (29) and (58), \mathbf{B}^H in (56) can be rewritten as

$$\mathbf{B}^H = \sum_{j=1}^{N_R} \mathbf{L}^{-1} \mathbf{D}^{-1} \mathbf{L}^{-H} \mathbf{S}_j^T \mathbf{S}_j \mathbf{L}^H \mathbf{S}_j^T \mathbf{S}_j \mathbf{D} \mathbf{e}_j \mathbf{e}_j^T = \mathbf{L}^{-1} \quad (59)$$

where we applied $\mathbf{L}^{-\text{H}} \mathbf{S}_j^{\text{T}} \mathbf{S}_j \mathbf{L}^{\text{H}} \mathbf{S}_j^{\text{T}} \mathbf{S}_j = \mathbf{S}_j^{\text{T}} \mathbf{S}_j$ which can be easily proved similar to Lemma 4. Using (29) and (59), the forward filter in (55) can be also simplified and we get (30).

Using (55) and (28), the error covariance matrix in (52) can be expressed in terms of \mathbf{B}^{H} as follows:

$$\Phi_{\varepsilon\varepsilon} = \gamma^{-2} \Phi^{-1} \mathbf{P}^{\text{T}} \mathbf{B}^{\text{H}} \Phi_{vv} \mathbf{B} \mathbf{P} \Phi^{-1} + \beta^{-2} \Phi_{nn}. \quad (60)$$

From (26), (28), and (55), the trace of the noise covariance matrix can be written as

$$\text{tr}(\Phi_{nn}) = \gamma^{-1} \beta^2 \text{tr}(\mathbf{H}^{\text{H}} \Phi^{-1} \mathbf{P}^{\text{T}} \mathbf{B}^{\text{H}} \Phi_{vv} \mathbf{B} \mathbf{P} \Phi^{-1} \mathbf{H}). \quad (61)$$

From (60) and (61), the MSE in (25) can be computed as

$$\begin{aligned} \varphi &= \gamma^{-2} \text{tr}(\Phi^{-1} \mathbf{P}^{\text{T}} \mathbf{B}^{\text{H}} \Phi_{vv} \mathbf{B} \mathbf{P} \Phi^{-1}) \\ &\quad + \gamma^{-1} \text{tr}(\mathbf{H}^{\text{H}} \Phi^{-1} \mathbf{P}^{\text{T}} \mathbf{B}^{\text{H}} \Phi_{vv} \mathbf{B} \mathbf{P} \Phi^{-1} \mathbf{H}) \\ &= \gamma^{-1} \text{tr} \left(\Phi^{-1} \mathbf{P}^{\text{T}} \mathbf{B}^{\text{H}} \Phi_{vv} \mathbf{B} \mathbf{P} \Phi^{-1} \left(\gamma^{-1} \mathbf{I}_{N_{\text{R}}} + \mathbf{H} \mathbf{H}^{\text{H}} \right) \right) \\ &= \gamma^{-1} \text{tr}(\Phi_{vv} \mathbf{B} \mathbf{P} \Phi^{-1} \mathbf{P}^{\text{T}} \mathbf{B}^{\text{H}}). \end{aligned} \quad (62)$$

With (29) and (30), (62) is finally simplified to (31).

REFERENCES

- [1] G. J. Foschini and M. J. Gans, "On limits of wireless communications in a fading environment when using multiple antennas," *Wireless Personal Commun.*, vol. 6, no. 3, pp. 311–335, Mar. 1998.
- [2] J. Jaldén and B. Ottersten, "On the complexity of sphere decoding in digital communications," *IEEE Trans. Signal Process.*, vol. 53, no. 4, pp. 1474–1484, Apr. 2005.
- [3] E. Viterbo and J. Boutros, "A universal lattice code decoder for fading channels," *IEEE Trans. Inf. Theory*, vol. 45, no. 5, pp. 1639–1642, Jul. 1999.
- [4] D. Seethaler, G. Matz, and F. Hlawatsch, "An efficient MMSE-based demodulator for MIMO bit-interleaved coded modulation," in *Proc. IEEE Global Telecommunications Conf.*, Nov./Dec. 2004, vol. 4, pp. 2455–2459.
- [5] P. W. Wolniansky, G. J. Foschini, G. D. Golden, and R. A. Valenzuela, "V-BLAST: An architecture for realizing very high data rates over the rich-scattering wireless channel," in *Proc. URSI Int. Symp. Signals, Systems, and Electronics*, Sep. 1998, pp. 295–300.
- [6] S. B aro, G. Bauch, A. Pavlic, and A. Semmler, "Improving BLAST performance using space-time block codes and turbo decoding," in *Proc. IEEE Global Telecommunications Conf.*, Nov./Dec. 2000, vol. 2, pp. 1067–1071.
- [7] A. Benjebbour, H. Murata, and S. Yoshida, "Comparison of ordered successive receivers for space-time transmission," in *Proc. IEEE Vehicular Technology Conf.*, Atlantic City, NJ, Oct. 2001, pp. 2053–2057.
- [8] D. W ubben, R. B ohnke, J. Rinas, V. K uhn, and K. D. Kammeyer, "Efficient algorithm for decoding layered space-time codes," *IEE Electron. Lett.*, vol. 37, no. 22, pp. 1348–1350, Oct. 2001.
- [9] D. W ubben, J. Rinas, R. B ohnke, V. K uhn, and K. D. Kammeyer, "Efficient algorithm for detecting layered space-time codes," in *Proc. 4th ITG Conf. Source and Channel Coding*, Berlin, Germany, Jan. 2002, pp. 399–405.
- [10] W. Zha and S. D. Blostein, "Modified decorrelating decision-feedback detection of BLAST space-time system," in *Proc. IEEE Int. Conf. Communications*, New York, Apr./May 2002, vol. 1, pp. 335–339.
- [11] R. B ohnke, D. W ubben, V. K uhn, and K. D. Kammeyer, "Reduced complexity MMSE detection for BLAST architectures," in *Proc. IEEE Global Telecommunications Conf.*, San Francisco, CA, Dec. 2003, vol. 4, pp. 2258–2262.
- [12] D. W ubben, R. B ohnke, V. K uhn, and K. D. Kammeyer, "MMSE extension of V-BLAST based on sorted QR decomposition," in *Proc. IEEE Vehicular Technology Conf.*, Oct. 2003, vol. 1, pp. 508–512.
- [13] B. Hassibi, "An efficient square-root algorithm for BLAST," in *Proc. IEEE Int. Conf. Acoustics, Speech, and Signal Processing*, Istanbul, Turkey, Jul. 2000, vol. 2, pp. II737–II740.
- [14] E. Biglieri, G. Taricco, and A. Tulino, "Decoding space-time codes with BLAST architectures," *IEEE Trans. Signal Process.*, vol. 50, no. 10, pp. 2547–2552, Oct. 2002.
- [15] J. Benesty, Y. A. Huang, and J. Chen, "A fast recursive algorithm for optimum sequential signal detection in a BLAST system," *IEEE Trans. Signal Process.*, vol. 51, no. 7, pp. 1722–1730, Jul. 2003.
- [16] R. Fischer, C. Windpassinger, A. Lampe, and J. Huber, "Space-time transmission using Tomlinson–Harashima precoding," in *Proc. 4th ITG Conf. Source and Channel Coding*, Berlin, Germany, Jan. 2002, pp. 139–147.
- [17] M. Tomlinson, "New automatic equaliser employing modulo arithmetic," *Electron. Lett.*, vol. 7, no. 5/6, pp. 138–139, Mar. 1971.
- [18] H. Harashima and H. Miyakawa, "Matched-transmission technique for channels with intersymbol interference," *IEEE Trans. Commun.*, vol. 20, no. 4, pp. 774–780, Aug. 1972.
- [19] R. Hunger, F. A. Dietrich, M. Joham, and W. Utschick, "Robust transmit zero-forcing filters," in *Proc. ITG Workshop on Smart Antennas*, Mar. 2004, pp. 130–137.
- [20] A. Scaglione, P. Stoica, S. Barbarossa, G. B. Giannakis, and H. Sampath, "Optimal designs for space-time linear precoders and decoders," *IEEE Trans. Signal Process.*, vol. 50, no. 5, pp. 1051–1064, May 2002.
- [21] G. Ginis and J. M. Cioffi, "A multi-user precoding scheme achieving crosstalk cancellation with application to DSL systems," in *Proc. Asilomar Conf. Signals, Systems, and Computers*, Oct. 2000, vol. 2, pp. 1627–1631.
- [22] R. F. H. Fischer, C. Windpassinger, A. Lampe, and J. B. Huber, "MIMO precoding for decentralized receivers," in *Proc. IEEE International Symp. Information Theory*, Jun./Jul. 2002, p. 496.
- [23] J. Liu and A. Duel-Hallen, "Tomlinson–Harashima transmitter precoding for synchronous multiuser communications," presented at the 37th Annu. Conf. Information Science and Systems, Mar. 2003.
- [24] M. Joham, J. Brehmer, and W. Utschick, "MMSE approaches to multiuser spatio-temporal Tomlinson–Harashima precoding," in *Proc. 5th ITG Conf. Source and Channel Coding*, Erlangen, Germany, Jan. 2004, pp. 387–394.
- [25] M. Joham, W. Utschick, and J. A. Nossek, "Linear transmit processing in MIMO communications systems," *IEEE Trans. Signal Process.*, vol. 53, no. 8, pp. 2700–2712, Aug. 2005.
- [26] M. R. Gibbard and A. B. Sesay, "Asymmetric signal processing for indoor wireless LAN's," *IEEE Trans. Vehicular Technol.*, vol. 48, no. 6, pp. 2053–2064, Nov. 1999.
- [27] L. L. Scharf, *Statistical Signal Processing*. Reading, MA: Addison Wesley, 1991.
- [28] G. Ginis and J. M. Cioffi, "On the relation between V-BLAST and the GDFE," *IEEE Commun. Lett.*, vol. 5, no. 9, pp. 364–366, Sep. 2001.
- [29] R. Fletcher, *Practical Methods of Optimization*. New York: Wiley, 1987.
- [30] S. Boyd and L. Vandenberghe, *Covex Optimization*. Cambridge, U.K.: Cambridge Univ. Press, 2004.
- [31] G. H. Golub and C. F. V. Loan, *Matrix Computations*, 3rd ed. Baltimore, MD: Johns Hopkins Univ. Press, 1996.
- [32] G. J. Foschini, G. D. Golden, R. A. Valenzuela, and P. W. Wolniansky, "Simplified processing for high spectral efficiency wireless communication employing multi-element arrays," *IEEE J. Sel. Areas Commun.*, vol. 17, no. 11, pp. 1841–1852, Nov. 1999.
- [33] M. Schubert and S. Shi, "MMSE transmit optimization with interference pre-compensation," in *Proc. IEEE Vehicular Technology Conf.*, May/Jun. 2005, vol. 2, pp. 1550–2252.
- [34] A. Mezghani, R. Hunger, M. Joham, and W. Utschick, "Iterative THP transceiver optimization for multi-user MIMO systems based on weighted sum-MSE minimization," presented at the SPAWC, Jul. 2006.



Katsutoshi Kusume (M'05) was born in Tokyo, Japan, 1974. He received the M.Sc. degree in communications engineering from the Munich University of Technology (TUM), Munich, Germany, in 2001, where he is currently pursuing the Ph.D degree.

In 2002, he joined DoCoMo Euro-Labs, Munich. His research interests include multiple antenna systems, multicarrier transmissions, iterative multiuser detection techniques, and *ad hoc* networking.

Mr. Kusume received the Werner von Siemens Excellence Award for his M.S. thesis in 2002.



Michael Joham (S'99–M'05) was born in Kufstein, Austria, 1974. He received the Dipl.-Ing. and Dr.-Ing. degrees (both *summa cum laude*) in electrical engineering from the Munich University of Technology (TUM), Munich, Germany, in 1999 and 2004, respectively.

Dr. Joham was with the Institute of Circuit Theory and Signal Processing, TUM, from 1999 to 2004. Since 2004, he has been with the Associate Institute for Signal Processing, TUM, where he is currently a Senior Researcher. In the summers of 1998 and 2000, he visited Purdue University, West Lafayette, IN. His main research interests are estimation theory, reduced-rank processing, and precoding in mobile communications.

Dr. Joham received the VDE Preis for his diploma thesis in 1999 and the Texas-Instruments-Preis for his dissertation in 2004.



Wolfgang Utschick (M'97–SM'06) completed several industrial education programs before he received the diploma and doctoral degrees, both with honors, in electrical engineering from the Munich University of Technology (TUM), Munich, Germany, in 1993 and 1998.

He has held a scholarship from the Bavarian Ministry of Education for exceptional students and a scholarship from Siemens AG. In 1993, he became a part-time Lecturer at the Technical School for Industrial Education. From 1998 to 2002, he was

Co-Director of the Signal Processing Group, Institute of Circuit Theory and Signal Processing, TUM. Since 2000, he has been instrumental in the Third Generation Partnership Project as an Academic Consultant in the field of multi-element antenna wireless communication systems. In October 2002, he was appointed Professor at the TUM, where he is Head of the Associate Institute for Signal Processing. His research interests are in signal processing, communications, and applied mathematics in information technology.

Dr. Utschick is a senior member of the VDE/ITG. He is an Associate Editor of the IEEE TRANSACTIONS ON CIRCUITS AND SYSTEMS—PART II: EXPRESS BRIEFS.



Gerhard Bauch (S'99–M'01–SM'05) received the Dipl.-Ing. and Dr.-Ing. degrees in electrical engineering from the Munich University of Technology (TUM), Munich, Germany, in 1995 and 2001, respectively, and the Diplom-Volkswirt degree from the FernUniversität Hagen in 2002.

In 1996, he was with the German Aerospace Center (DLR), Oberpfaffenhofen, Germany. From 1996 to 2001, he was a member of scientific staff at TUM. In 1998 and 1999, he was a Visiting Researcher at AT&T Labs Research, Florham Park, NJ.

In 2002, he joined DoCoMo Euro-Labs, Munich, where he is currently Manager of the Advanced Radio Transmission Group. Since October 2003, he has also been an Adjunct Professor at TUM. His research interests include channel coding, turbo processing, multihop transmission, and various aspects of signal processing in MIMO.

Dr. Bauch received the best paper award from the European Personal Mobile Communications Conference (EPMCC) 1997, the Texas Instruments award from TUM, and the award from the German Information Technology Society (ITG in VDE) (ITG Förderpreis).